Similar-Sized Collisions and the Diversity of Planets

Erik Asphaug

October 11, 2009

Earth and Planetary Sciences Dept.
University of California
1156 High St.
Santa Cruz, CA 95064
USA
easphaug@ucsc.edu
phone: (831) 459-2260
fax: (831) 459-3074

Abstract

It is commonly assumed in models of terrestrial planet formation that colliding bodies simply merge. From this the dynamical and chemical properties (and potential for life) of finished planets have been computed, and our own and other planetary systems compared to the results of N-body integrations. But simple analyses and detailed models show that mergers are exceptions to the rule, for the similar-sized collisions that dominate terrestrial planet formation. Moderately off-axis SSCs are grazing, in that their centers of mass overshoot at typical impact parameters. Averaged over impact parameter, by far the most common outcome for impact velocities $\sim 1.1\, v_{esc}$ to $\sim 3\, v_{esc}$ is "hit-and-run", where the impactor skips off but is profoundly deformed and altered by shears, shocks, tides and torques. Highly grazing SSCs strip off the outer layers of the impactor and cause global unloading from hydrostatic pressure, with small damage to the target. Even 30° from normal can be a glancing blow, shearing an unaccreted impactor into a chain of sizable new planetoids of grossly varying bulk composition, and causing intense shock damage to the impactor and target. What emerges from this modeling is a hypothesis for planetary diversity that applies to the largest bodies that have something larger to run into – the next largest bodies within a factor of ~ 3 in size. Most of these eventually get accreted, but since hit-and-run is a more likely outcome than efficient merger, they undergo one or two hit-and-run collisions first. Those that survived the attrition of mergers experienced numerous hit and run episodes by the end of planet formation, driving them towards exotic composition and evolution. Mercury and many of the meteorite parent bodies in the Main Belt are unaccreted survivors of such an epoch, and have been torn apart by their encounters with larger planets. In solar systems with super-Earths, profound diversity is predicted among their Earth-mass planets, the majority of which will be devoid of atmospheres and oceans and have highly processed outer mantles – the consequence of non-accretionary collisions with super-Earths.

1 Introduction

During terrestrial planet formation most of the colliding matter comes late, in the form of similar-sized bodies encountering at speeds from 1 to a few times their mutual escape velocity v_{esc} (Wetherill, 1985). Here I review what is essentially an edge effect that occurs under planet-forming conditions, where the "next-largest" bodies in a hierarchically-accreting population – those a few times smaller than the largest, an order of magnitude more numerous – grow increasingly exotic every time they collide with a larger body but do not accrete. This happens commonly. These outcomes are highly diverse next-largest planets – whether they be dwarf planets in our solar system, or Earth-mass planets in systems with super-Earths, or the next-largest members of an accreted satellite population.

Collisions involving bodies within a factor of $2-3$ in size are extended-source phenomena. Also, when the random velocity $v_\infty \approx v_{esc}$ the contact and compression timescale of projectile deformation equals the gravity timescale, which is very different from what we are used to in impact cratering mechanics. Moreover, for typical geometries only a fraction of the colliding matter intersects – the rest goes sailing on, as it were, and the abrupt shears and unloading stresses unleash a host of planetary processes, some rather novel to consider. Similar-sized collisions (SSCs) are thus phenomelologically much different than impact cratering, for which events are usually treated as a point-source, where contact and compression occurs orders of magnitude faster than gravitational modification and ejecta evolution, and where the discrete fate of the bullet is not of great significance except under the most oblique incidence (Pierazzo and Melosh, 1999).

For SSCs the fate of the bullet is of *principal* consequence, even for modest impact angles. The best-studied archetype of a similar-sized collision is the giant impact hypothesis for the origin of the Moon, so let's begin there. In this scenario the bullet gets shredded into two components, its core which merges with the center of the Earth, and its mantle which interplays with Earth's outer mantle to form a protolunar disk of several lunar masses (e.g. Stevenson, 1987; Benz *et al.*, 1989; Canup and Asphaug, 2001). This gross fractionation of the bulk Moon from the bulk Earth, forming a new minor planet lacking in iron and volatiles, is closely analogous to how SSCs leave their permanent and formative imprint upon minor worlds and their bulk composition.

Giant impacts such as the Moon's formation are high energy end-members of SSCs. The phenomenon scales down to smaller colliding pairs impacting at correspodingly lower velocity – for instance, Vesta-sized molten planetesimals colliding during the early epoch when the largest bodies were $\lesssim$ 1000 km diameter, at random speeds comparable to their smaller v_{esc}, a few 100 m/s. The manner in which planets of different sizes and stages of accumulation respond differently during SSCs is a main focus of this review, which looks at planet formation, asteroid parent body formation, and early chemistry.

Although it is widely assumed in numerical integrations of planet formation that similar-sized

collisions result in effective mergers, this is very far from true. Based on numerical impact simulations about 2/3 of SSCs are hit-and-run, for typical random velocities $0.7\,v_{esc} \lesssim v_\infty \lesssim 2.5\,v_{esc}$. That is to say, for every merger into one of the largest bodies, there will be one or two hit-and-run collisions, assuming a nominally stirred-up population. If so, then unaccreted bodies within a factor ~ 3 in size of the largest become exotic and diverse in finished solar systems, in the manner explored below, with implications for the Moon, Mercury, the parent bodies of the Main Belt, accretionary satellite systems, and for Earth-mass planets in systems with super-Earths.

2 Similar Sized Collisions

Most of the colliding mass striking an accreting planet comes by way of the largest impacts, bodies within an order of magnitude in mass that have been stirred up gravitationally to around the dominant planet's escape velocity (Wetherill, 1985; Agnor *et al.*, 1999). This is sometimes called the late stage, but collisions involving similar-sized bodies dominate earlier phases of planet formation as well. Morbidelli *et al.* (2009) conjecture, on the basis of planetesimal accretion models by Johansen *et al.* (2007); Cuzzi *et al.* (2008) and others, that planetesimals might bypass hierarchical growth entirely, accreting directly from the nebular dust and gas, thereby avoiding the long-perplexing small-size bottleneck, which arises in models (Benz, 2000; Leinhardt *et al.*, 2000) that show that small bodies would bash one another apart in random collisions much more frequently than mergers. In order to explain the apparent factor of 4 overabundance of 100 km asteroids in the present main belt, Morbidelli *et al.* argue that asteroids were "born big", 100 km diameter or larger.

Perhaps so. Even in the case of hierarchical growth and a power law distribution of sizes, most of the mass colliding interacts at the large end of the feeding chain, so that impacts are dominated by SSCs between the largest and the next-largest bodies. Consider a size distribution

$$N(r) \propto r^{-\beta} \tag{1}$$

where N is the cumulative number of planetesimals larger than r. In the case $\beta = 4$ there is equal mass in equal logarithmic bins, i.e. equal mass in bodies 100's of km diameter as in bodies meters in diameter. But observed planetesimal size distributions are considerably shallower, with almost all mass in the largest bodies. In the present Main Belt, the four largest asteroids, within a factor of 2 in diameter, account for half the total mass of the population.

On average, the present Main Belt asteroids follow $\beta \sim 2 - 3$, varying with size and subpopulation. Recently disrupted comet groups and the comet population as a whole appear to have $\beta \sim 1.7$ (see Weissman *et al.*, 2004). For a ground-down population obeying size-independent fragmentation physics, the theoretically derived equilibrium value is $\beta = 1.83$ (Dohnanyi, 1969). Gravitational focusing and oligarchic sweep up of feeding zones shifts the mass into larger sizes

Kokubo and Ida (1998). For characteristic minor planet and small body populations, most of the mass (and hence most of the colliding mass) is found in the handful of largest bodies, whether they are born big or become big.

2.1 Colliding Pairs

In their studies of the evolving Main Belt asteroid size distribution, Bottke *et al.* (2005); Morbidelli *et al.* (2009) consider impactors up to the size of the target, statistically following the erosional and disruptive evolution of candidate primordial Main Belts to see which ancestral size distribution could have led to the population now observed. Their models consider impactors up to the size of a given target, but no larger – a seemingly obvious choice given that small asteroids are usually demolished by smaller members of the population, since the random velocities orders of magnitude faster than the escape velocities. Indeed, demolition by an equal sized body seems exotic.

But for the largest asteroids, even at modern solar system velocities, the impactors required to disrupt them can be as big as they are. Figure 1 shows a differentiated planet 500 km diameter, consisting of 30:70 by mass of iron and silicate, being impacted by a 200 km diameter rocky asteroid at 10 km/s (top four panels) and 5 km/s (bottom two panels) at impact angle $\theta = 45°$. The 10 km/s impact, at ~2-3 times the velocity that is typical of the modern Main Belt and ~ 30 times the mutual escape velocity of the pair, barely does the job of leaving half the mass behind (the definition of catastrophic disruption). The 5 km/s impact, at a more typical velocity, does little more than blast off the crust.

Once asteroids grow large, they seem to become difficult or impossible to wholly disrupt without invoking extreme circumstances (see also Scott *et al.*, 2001). But they are not so difficult to disrupt if they hit something larger than themselves. The next-largest bodies can, perhaps, be ripped to pieces in hit and run collisions more easily than they are bashed to pieces by an impactor. And so, in a scenario drawn from some of the simulations reviewed below, a dozen 200 km asteroids might result from the hit-and-run breakup of a single Vesta-sized asteroid that was dashed at a few km/s against a long-gone (scattered or accreted) Moon-sized world. Returning to the conclusions of Bottke *et al.* (2005); Morbidelli *et al.* (2009), that the ~ 100 km bodies must be primordial, this might not be the case if one accounts for all of the unaccreted impactors that are torn apart.

A different kind of modeling approach for studying planet formation is to build up rather than break down a primordial population, using accretion codes that apply advanced N-body computational methods to directly integrate the orbits and interactions of planets and asteroids around the Sun. Out of computational necessity these codes assume the simplest possible collisional physics – usually the perfect merger – in order to track millions of years of mergers to form finished terrestrial planets. The usual assumption is that planets of mass M, m and radius R, r stick when they hit, forming a larger sphere of mass $M + m$ that conserves linear and angular momentum.

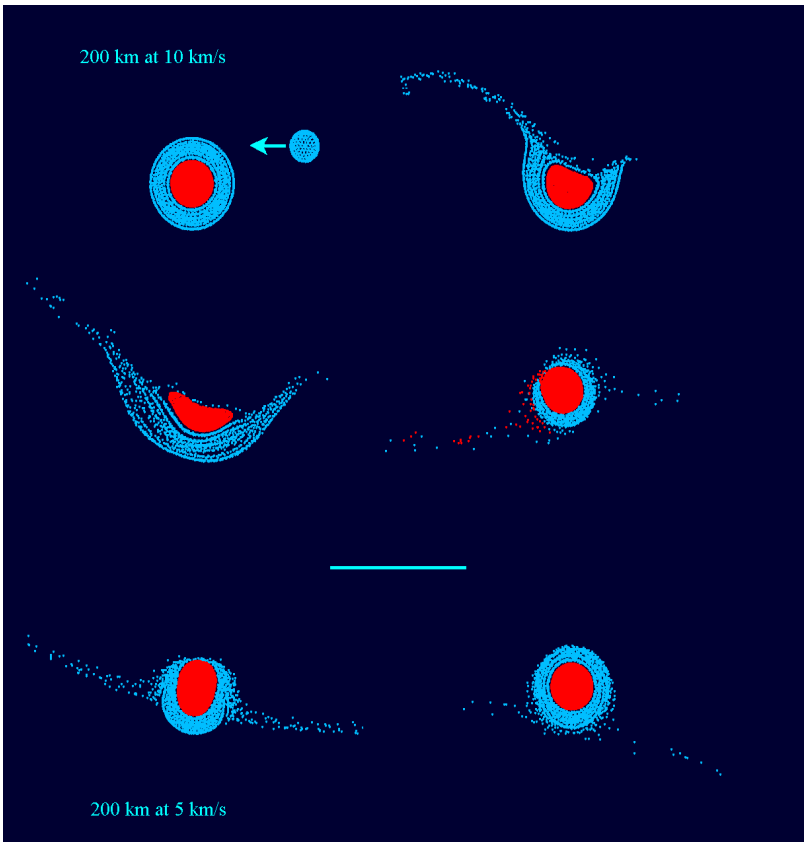

Figure 1: Disruption of a Vesta-type (500 km differentiated) asteroid by a 200 km diameter rocky body at 10 km/s (top four frames) and at 5 km/s (bottom four frames), in the target-center frame. Simulations by Craig Agnor (Asphaug and Agnor, 2005). The goal of this suite of simulations was to study the problem of liberating core material from a differentiated large asteroid (a problem studied byScott *et al.* 2001 concerning the origin of mesosiderites). Each case is for the typical impact angle $\theta = 45°$. Snapshots for $v_{imp} = 10$ km/s are plotted before and at t =120, 390, and 12,000 seconds after contact in the top four frames, and for $v_{imp} = 5$ km/s at $t = 390$ and 12,000 seconds in the bottom frames. The slower impact (typical of contemporary Main Belt collisions) is still $\sim 15 \times v_{esc}$ and only removes the top third of the mantle. The 10 km/s impact is at $\sim 30 \times v_{esc}$ and barely does the job of exposing core iron to the surface, let alone stripping off the mantle. The core iron is deeply sheltered and hasgreat binding energy. The results deepen the quandary of how Vesta, which retained a thick basaltic crust, did so while dozens of other differentiated asteroids were disrupted to their core. If would seem to have dodged quite a fusillade; however, the results inevitably lead us to contemplate impactors larger than the target turning the problem on its head, and causing us to leave this target-centric frame of reference behind. [Print in color.]

Encounters are treated as perfectly elastic gravitational encounters if the impact parameter $b > R+r$ (no mass transfer), and are perfectly inelastic mergers if $b \leq R+r$, in which case accretion efficiency is assumed to be $\xi = 1$, as defined below.

In such simulation methods a lot more effort has gone towards achieving numerically precise dynamical integration of gravity and close gravitational encounters, than towards accurately modeling the outcomes of colliding planets. Because only a few hundred particles can be evolved with high precision for the required $\sim 1-100$ Ma, this does not allow for a great range in size in explicit N-body integrations, and thus in all collisional cases $r \sim R$. The most detailed N-body accretion simulations published so far range from Moon sized to Earth sized bodies, a range in mass of ~ 100. Every collision is therefore an SSC, yet the standard assumption is perfect merger.

Among other things, this assumption bestows upon planets a capacity for arbitrary amounts of spin angular momentum – an aspect that was proven untenable by Agnor *et al.* (1999), who tracked angular momentum during typical terrestrial planet-forming calculations and found that finished planets in such simulations rotate with periods as short as $1-2$ hr. This is close to or exceeds dynamical stability (Chandrasekhar, 1969); moreover such rapid spins would have to be slowed down to present-day rotations by some mechanism, such as loss of a large satellite, or spin-orbit coupling with another planet or its core.

The obvious solution appears to be that collisions that bring in too much angular momentum have close to zero accretion efficiency – the bodies do not merge even though $b < R + r$, thereby limiting the accumulation of spin. This is true whether angular momentum comes in the bodies' own rotations, or (usually much greater) in the collision angular momentum $m\overrightarrow{v} \times \vec{\mathbf{b}}$, where $\vec{\mathbf{b}}$ is the impact vector at collision (the impact parameter) and $m\overrightarrow{v}$ the momentum. The total collisional angular momentum is lowest for small b (direct hits) and small v. Without doing any calculations one can surmise that fast, grazing impacts do not contribute greatly to accretion. How fast, and how grazing, is quantified below.

2.2 Scale Invariance

It is useful to think about the scale invariance of similar-sized collisions. While the numerous departures from invariance provides the framework for of Section 3, strict invariance does apply in the limit of incompressible, self-gravitating inviscid fluid planets. So, for example two 100 m diameter ideal spheres colliding at $v_{imp} = 30$ cm/s (a few $\times$ their v_{esc}) are indistinguishable from two 1000 km ideal spheres of the same density colliding at $v_{imp} = 30$ km/s, when velocities are scaled to the relative escape velocity

$$v_{esc} = \sqrt{2G(M+m)/(R+r)} \tag{2}$$

and distances are scaled to the size of the bodies. This is the same as equating the collision timescale

$$\tau_{coll} = 2r/v_{imp} \tag{3}$$

to the gravitational (self-orbiting) timescale

$$\tau_{grav} = \sqrt{3\pi/G\rho} \tag{4}$$

where the two colliding spheres are of mass $M \gtrsim m$ and radius $R \gtrsim r$, and uniform density $\rho = M/\frac{4}{3}\pi R^3 = m/\frac{4}{3}\pi r^3$. The collision time, or contact and compression time (Melosh, 1989), is the time it takes a colliding body to cross its own diameter. If this is held at a fixed proportion to τ_{grav} – equivalent to holding v_{imp} at fixed proportion to v_{esc}, e.g. a constant Safronov number (see below) – then the collisions are invariant for a given value of density, impact angle, and pre-impact rotation rate.

The notion of scale invariance is ideal, as planets are compressible, and indeed rheologically and thermodynamically complex. It is quite plausible that silicate melts are likely to be found deep inside any 100 km diameter or larger early-stage terrestrial body. At high interior pressures these melts are very soluble to water and other volatiles. In contrast, sub-kilometer bodies are unlikely to retain any appreciable melt or dissolved gas at any stage in their formation or evolution – they are too small to retain heat and too underpressured to retain gas. These smallest bodies (typical asteroids and comets) are likely to behave as solids or granular solids during collisions, obeying a physics perhaps akin to landslides.

Large molten planets become differentiated, with iron towards the core and lighter mantle- and crust-forming materials in the outer regions. This increases their global binding energy and perches the volatiles and silicates at the lowest binding energy. Their cores and deep mantles become sheltered from disruptive collisions, as was demonstrated in Figure 1. Unmelted or primitive bodies, on the other hand, retain a more homogeneous composition and a lower overall binding energy, and have been found in models run alongside those shown in Figure 1 to be almost 3 times easier to disrupt, in terms of required impact energy, compared to differentiated planets. It is truly an enigma that iron should be the most tighly-bound accreted material, yet the most common representative of our meteorite collections – a topic discussed further in the context of hit-and-run collisions and the basaltic crust of Vesta.

For the reasons described, scale-invariance provides first-order physical insight rather than a fast rule. Foremost it allows us to define a class of planetary collisions, SSCs, where the impactor and target are of similar size, and where the random velocity v_∞ is similar to the escape velocity v_{esc}. In the context of classic accretion theory (reviewed in Wetherill, 1980), scaling the random velocity to the escape velocity is the same as assuming a constant Safronov number

$$\Theta = \frac{v_{esc}^2}{2v_\infty^2} \tag{5}$$

It was originally proposed by Safronov and Zvjagina (1969) that $\Theta \approx 1$ in the case of orderly growth, where random velocities are the result of gravitational stirring by the dominant members of the accreting population. The basic reasons are that close passages with the largest bodies are common, so that velocities become randomized to v_{esc}, and that random velocities of the stable population do not grow much beyond this value.

If we restrict ourselves to inviscid, molten, differentiated colliding pairs – astrophysical rather than geological objects – then the most basic assumptions of scale invariance are met. But even then there are important differences at the largest scales arising from powerful shocks and high hydrostatic pressures, which can lead to different outcomes. Large SSCs (a.k.a. giant impacts) are hypervelocity because $\sqrt{2GM/R}$ exceeds the sound speed of the colliding materials; they are shock-inducing collisions leading to global-scale internal heating and Hugoniot acceleration.

The other major factor is that H_2O and CO_2 solubility in silicate melts is greatly enhanced at high interior pressures (e.g. Dixon *et al.*, 1988). When a large planetesimal loses its "lid" (Figure 2) then its volatile-rich pressurised materials (a few wt% H_2O may be typical) can erupt violently, being released over τ_{grav} from a hydrostatic pressure P, which can be of a magnitude and timescale (kilobars, hours) that are comparable to gas-driven kimberlite eruptions on Earth (Kelley and Wartho, 2000; Porritt and Cas, 2009; Kamenetsky *et al.*, 2007). As shown below in a study of purely tidal collisions, even a non-impacting impactor can lose much of its outermost mass and have its central pressure lowered by half for an hour, at a rate of pressure release

$$\dot{P} \sim P_o/\tau_{grav} \sim r^2 \tag{6}$$

and by ~20% permanently. The pressure release adds $V\Delta P$ to the available specific enthalpy $\Delta h = \Delta u + P\Delta V + V\Delta P$ where volumetric expansion $P\Delta V$ occurs especially in the case of bubble formation(Gardner *et al.*, 1999).

2.3 Collisional Geometry

In impact cratering the impactor gets rapidly buried into a semi-infinite target and effectively explodes, coupling as a point source without much downrange ballistic motion. The impact angle can therefore be parameterized with good results, as there is little difference to the physics except for the shallowest collisions (Pierazzo and Melosh, 1999). Similar-sized collisions, on the other hand are sensitive to impact angle over all ranges of θ. Additionally, because the impact timescale for SSCs is the same as the gravity timescale, gravitational deformation and instabilities can grow even during

contact and compression phase (to use the language of cratering), resulting in collisional outcomes that can resemble the outcomes of tidal disruption (linear chains of similar-sized fragments) and that can, for instance, segregate the core from the mantle of an impactor on the basis of density.

The sensitivity to impact angle can be understood in the following simple way. A similar-sized impactor does not have semi-infinite mass to bury itself into. Figure 1 shows how a large fraction of the mass "misses" the target, in the sense that there is no physical intersection along the trajectories at the time of impact, for all but the most direct hits. Impacts that in impact cratering would not be noticably oblique ($\theta \sim 30^\circ - 60^\circ$) are very much grazing when it comes to SSCs.

The probability of impact at an angle between θ and $\theta + d\theta$ by a point mass onto a spherical gravitating target is $\frac{1}{2}\sin^2\theta d\theta$, a function that peaks for impact angle $\theta = 45^\circ$ (Shoemaker, 1962); 45° is also the median impact angle. (The impact angle is, for undeformable colliding spheres, the same angle as that of a point mass at the impactor center impacting a virtual sphere of radius $R+r$, thus Shoemaker's original argument still applies.) If one defines impact parameter b (Figure 2) as the offset from the impactor trajectory from the target center of mass at the moment of collision, then $b = (r + R)\sin\theta$ and the most likely impact parameter is $b_{45} = (r + R)/\sqrt{2}$. Note that b is somewhat larger than the periapse that would be computed for a collisionless point-mass encounter, at the moment of periapse – in a giant collision, periapse is not well defined.

For impact cratering (small r/R) the traditional definition of grazing is $b = R$, where the impactor skims tangential to the target. For SSCs we can abstract this notion, so that the angle of grazing incidence is defined when the center of mass of the smaller colliding body is tangential to the larger:

$$\theta_b = \sin^{-1}\left(\frac{R}{R+r}\right) \tag{7}$$

(Figure 3). For equal sized planets $r = R$, and grazing as so defined requires angles no shallower than $\theta_b = 30^\circ$, not far from head-on. When $r = R/2$ grazing occurs for $\theta > \theta_b = 42^\circ$, more than half the time. For small r, the fraction f that is shaded grey in Figure 2 approaches a step function around $b = R$, corresponding to the fact that impact cratering into a halfspace is all-or-nothing, while for SSCs there is gradation over a broad range of angles.

If two differentiated planets with the same ratio of core radius r_{core} to planet radius r collide, then their cores miss one another entirely for

$$\theta_{core} > \sin^{-1}(r_{core}/r)$$

for any r, R (Figure 4). Among terrestrial planets $r_{core} \sim r/2$, so for any impact between 30° and

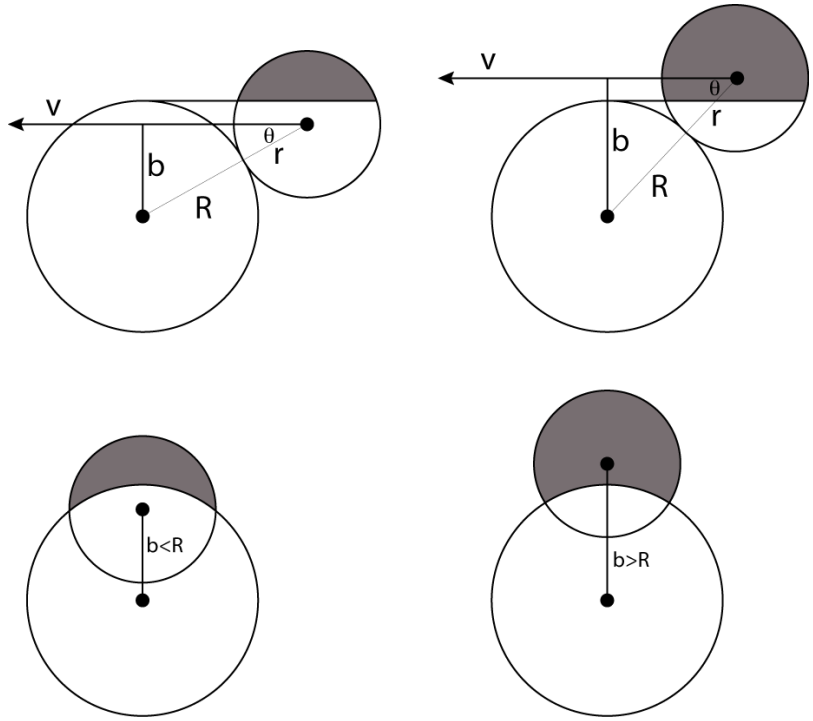

Figure 2: Impact geometry in similar-sized collisions, in side view and front view. Only a portion of the impactor intersects any mass of the target, and quite commonly, the center of mass overshoots, which is called grazing. For differentiated planets, their mantles might intersect but none of their cores. The smaller body (radius r) is by convention called the impactor, and the larger body (R) the target, but with $v_\infty \approx v_{esc}$ and $r \approx R$ this is more mechanics than ballistics. Shown are two bodies a factor of 4 different in mass ($r = 0.6\,R$, assuming $\rho_r = \rho_R$) at the moment of collision, where $\theta = 30°$ (left) and $\theta = 45°$ (right). At left the impact parameter $b < R$; at right $b > R$ in which case the center of mass misses the target. From a mechanical point of view, the "lid" (~1/3 the impactor mass at left; ~4/5 the impactor mass at right) gets sheared off of the smaller body as the inner portion abruptly decelerates. The non-colliding fraction of the impactor is shaded grey in the symmetry plane of each collision (top) and in the front-on view (bottom). The actual mechanics of hit-and-run is much more complex, involving gravitational stresses and torques and shocks, but this simple geomety explains why hit-and-run is more common than effective accretion under typical planet-forming conditions. It is important to recognize that half of all collisions are more grazing than the case to the right.

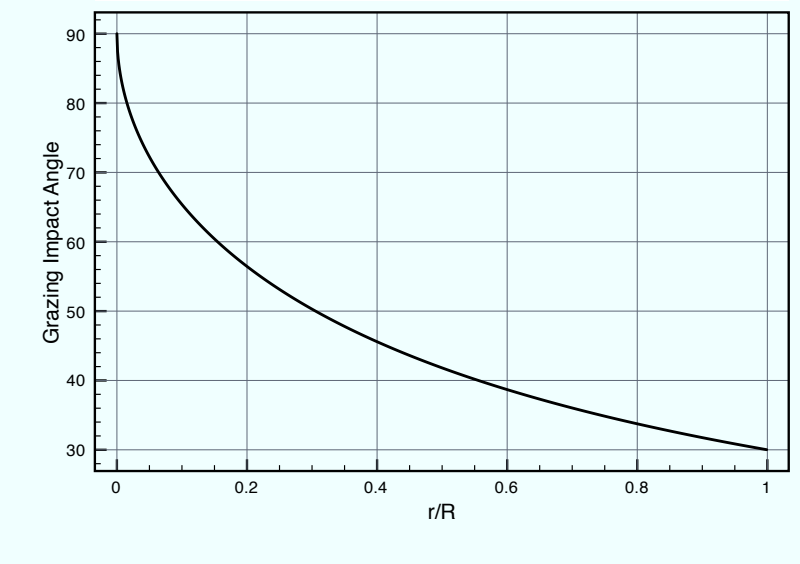

Figure 3: Grazing incidence angle as a function of relative sizes of the colliding pair r/R. Grazing is defined as a linear trajectory in which the center of mass of the impactor misses the target (see Figure 1). For relative size $r/R \gtrsim 0.4$ or relative mass $M \gtrsim 20\,m$ most collisions are grazing ($\theta_b \leq 45°$). Purely tidal (non-impacting) collisions are an important class of grazing collisions (see Figure 11) but are not included here as θ is undefined.

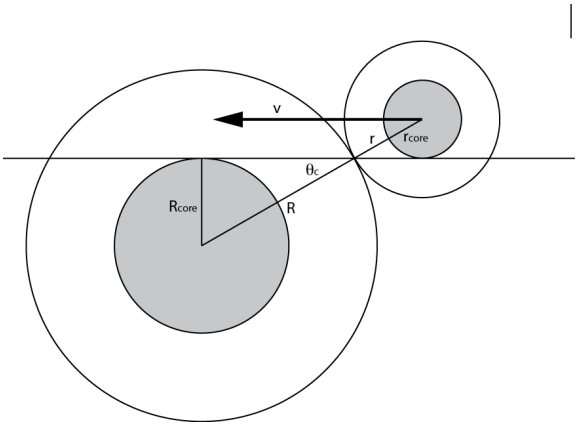

Figure 4: A collision with impact angle greater than $\theta_c = \sin^{-1}(r_{core}/r)$ may have little direct core-core interaction. The core in this case is half the radius, so that $\theta_{core} = 30°$. Impacts steeper than θ_{core} will trend towards great core interaction (and mergers for low velocity), while shallower impacts (most of them, that is) might have little core interaction. This is a question worthy of far more detailed hydrocode analysis.

90° the cores miss one another. While this is a simplistic approach to collisions, it does seem to make a sound prediction that the level of core-core interaction during giant impacts is highly variable, with some events shredding and intermingling mantle materials but not cores, and others merging cores entirely. Idealized assumptions about planetary collisions and their mixing are probably untenable; see Nimmo and Agnor (2008) for a discussion on this issue.

These are geometric idealizations. Fluid bodies begin to deform gravitationally hours before contacting, and are ellipsoidal by the time of their collision (e.g. Sridhar and Tremaine, 1992). Shoemaker's argument for impact angle will change, because impact angle is not well defined once the bodies deform tidally, and angular momentum goes into torques. Cores interact gravitationally with the mantles, which are about twice as massive, and can merge even if not headed at one another. Impact trajectory is not a straight line. The mass does not come off as a "lid". Lastly, there is no abrupt change in the physics of the encounter between a physical impact into some small fraction of the target ($b \lesssim r + R$) compared to a purely tidal collision that barely misses ($b \gtrsim r + R$), whereas the discussion of impact angle probability considers only those bodies which physically intersect. A purely tidal collision has enormous physical consequences to the impactor as reviewed below, and broadens the category of grazing events.

But this geometrical explanation provides a fundamental understanding for why hit-and-run collisions are so common. The preponderance of grazing impacts means that there are not two but *three* kinds of planetary collisions during accretionary epochs:

1. Accretionary collisions, which grow larger planets, and must at some point be dominant.

2. Disruptive collisions, which reverse the process of accretion and must at some point be minor.

3. Unaccretionary collisions, a.k.a. hit-and-run, which can strip, disrupt, or shred the unaccreted impactor.

While unaccretionary collisions may seem exotic, hit-and-run is in fact more common than effective accretion, for SSCs at typically stirred-up random velocities. It is argued that hit-and-run may dominate the physical and chemical evolution of the planetary bodies that grow large, but not largest, in terrestrial planet-forming settings.

2.4 Modeling Similar-Sized Collisions

Canup and Asphaug (2001) conducted a systematic study of potential Moon-forming collisions, based upon computer simulations using the smooth-particle hydrodynamics (SPH) method pioneered for giant impact studies by Benz *et al.* (1988); Cameron and Benz (1991) and others. We used a simple but appropriate nonlinear equation of state (Tillotson) for iron cores and rocky mantles, and set the random velocity to zero ($v_{imp} = v_{esc}$) in order to maximize the disk mass while satisfying the final system angular momentum. The impacts studied were otherwise characteristic of terrestrial planet-forming collisions.

In the course of this search for the best case scenario for late-stage Moon formation around proto-Earth, we made a few exploratory simulations with $v_\infty > 0$ and that some of these impacting planets were "skipping" from the target Earth. Indeed, the best case scenario identified for Moon formation turned out to be an impactor which almost, but not quite, skips off (see Figure 5). Only 30% faster and there would have been no Moon, but two planets – one still rather Earth-like, and the other one less massive than before, missing much of its mantle – resembling Mercury, perhaps.

Agnor and Asphaug (2004a) applied the same hydrocode method and equation of state to the general problem of similar-sized collisions, in a paper studying accretion efficiency between identical differentiated Mars-mass ($M = m = 0.1 M_\oplus$) terrestrial planets colliding at a range of possible impact angles, at velocities ranging from v_{esc} to $3\, v_{esc}$. Agnor and Asphaug (2004b) and Asphaug *et al.* (2006) broadened this suite of simulations to include SSCs among differentiated planets with mass ratios 1:10, 1:2 and 1:1 – impact conditions believed to be typical for the late stage of terrestrial planet formation (Wetherill, 1985; Agnor *et al.*, 1999). Our results are consistent with different SPH simulations by Marcus *et al.* (2009) using tabular equations of state and higher resolution, and thus appear to be robust.

SPH is a Lagrangian method that uses smoothed mass elements (spherical kernel functions) to compute the hydrodynamic and shock stresses and the pressure and gravity accelerations, and to track the trajectory and evolution of matter. SPH is very well suited to the computation of the total bound mass in a collisional system – or more generally, bound masses $M_1,\ M_2,\ M_3, ...$ where M_1 is the largest collisional remnant, M_2 the second largest, and so on (see e.g. Benz and

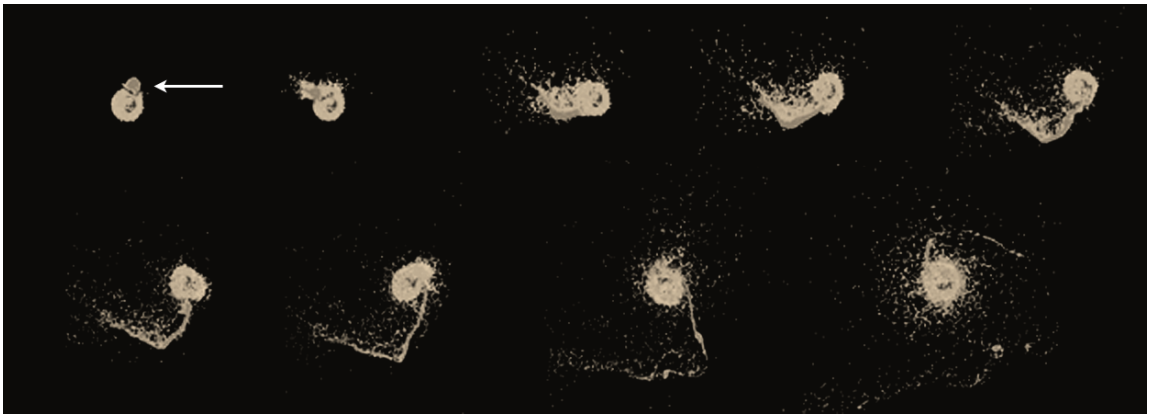

Figure 5: Hit and almost run. Moon formation in a late stage, lowest-velocity ($v_\infty = 0$) collision with proto-Earth, in a best-case giant impact scenario identified by Canup and Asphaug (2001). A proto-lunar disk of the appropriate mass, angular momentum and composition (greatly diminished in iron and volatiles) forms about the accreted Earth after the Mars-mass impactor ($0.1M_\oplus$, coming from the right) first bounces off the $0.9M_\oplus$ proto-Earth. The impactor, starting from zero potential, is captured and thereafter begins accreting ~4 hours after the initial contact, in the last four frames, after which point it is shredded by tidal and impact shears. The core merges with the Earth and the debris shears out into a protolunar disk of about 2 lunar masses in this simulation. Shown are times $t = 0.3$, 0.7, 1.4, 1.9, 3.0, 3.9, 5.0, 7.1, 11.6 hrs after initial contact. According to simulations at slightly higher impact velocity, these events more typically end with the impactor escaping as a novel planet; in this case it would be no longer Mars-like, and much more like Mercury. Print in greyscale.

Asphaug 1999). Prior to a collision, and in the limit of a non-collision, $M_1 = M$ and $M_2 = m$. The computation of the final gravitationally bound masses M_1 and M_2 is done as in Benz and Asphaug (1999), although it must be noted that reaccretion of this matter may occur much later, especially for large-scale events, as the escaping debris is now on a similar orbit around the Sun.

The determination of M_1 to 5% or better, is converged using modest ($\lesssim 10^5$) numbers of particles in a simulation. That is, the answer does not change with further increases in resolution, nor is the result very sensitive to the equation of state (e.g. Tillotson and ANEOS give very similar results). Thus the accretion efficiency

$$\xi = {}^{M_1 - M}/_{m} \tag{8}$$

is regarded in the simulations below to be determined to better than 10%. Here ξ is the mass gained or lost by the target planet $(M_1 - M)$ divided by the mass in the smaller planet (m) available for accretion. When $M_1 = M + m$ all of the impactor is accreted by the target ($\xi = 1$).

By comparison, modeling Moon formation using the same computational tools is a much bolder endeavor. Only a few percent of the collisional ejecta end up in orbit, conditions satisfied by a narrow range of ejection velocities between v_{orb} and $\sqrt{2}v_{orb} = v_{esc}$, where $v_{orb} = \sqrt{GM/a}$ and a is the radius of the protolunar disk that forms, outside the corotation radius. The dynamics must be evolved correctly for at least one orbital time in response to very near field gravitational torques, and the longer timescale and higher precisions required imply far great sensitivity to the equation of state (e.g. Canup, 2004) and to radiative evolution. The central issues posed in the review by Stevenson (1987) still stand.

2.5 Collisional Outcomes

Normalizing runs involving various mass ratios m/M of colliding pairs in terms of their accretion efficiency allows for different suites of SPH simulations to be plotted in the same graph. Figure 6 plots ξ as a function of impact velocity, for Mars-mass ($M = 0.1\,M_\oplus$) planets colliding with somewhat smaller planets ($m = 0.01M_\oplus$, $0.05M_\oplus$, $0.1M_\oplus$), at impact velocity between $v_{esc} \leq v_{imp} \leq 3\,v_{esc}$. The random velocity $v_\infty = (v_{imp}^2 - v_{esc}^2)^{1/2}$. Most Moon-forming simulations conducted to date are along the left axis. The simulations plotted are from Agnor and Asphaug (2004a,b). In all simulations the spatial resolution is $30,000$ particles, and the iron:silicate mass ratio is 70:30. Planets are hydrostatic and nonrotating prior to collision, and are placed initially at 5 R_{roche} to allow the pre-impact tidal strains to develop.

The impact angles 30°, 45°, 60°, 90° each represent approximately 1/4 of the impact probability for each colliding pair. It is readily apparent that the results are very sensitive to impact angle, and that even for relatively normal impact angles (30°) the influence of grazing is pronounced for common speeds, as expected on the basis of Figure 2. There are three branches of this plot,

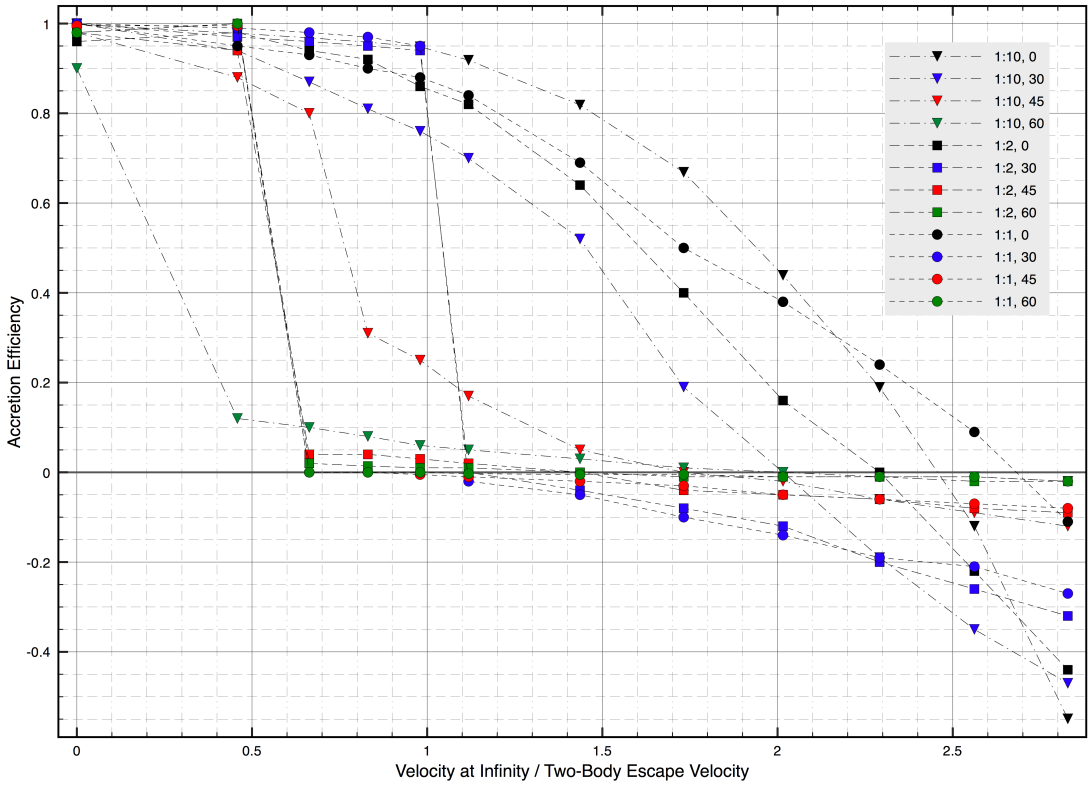

Figure 6: Accretion efficiency for colliding planetary pairs as a function of random velocity v_∞ and relative mass ratio and impact angle. Data from Agnor and Asphaug (2004a,b). Collisions occur between differentiated $M = 0.1\ M_\oplus$ (Mars-like) planets, and impactors ranging in mass $m = M,\ M/2,\ M/10$. Each angle represents about 1/4 of the probability interval of collisions $dP(\theta) = {}^1\!/_2 \sin^2\theta d\theta$, with 0° being head-on. Impact velocities v_{imp} in these simulations range from v_{esc} to $3\,v_{esc}$ and are plotted here as $v_\infty / v_{esc} = [(v_{imp}/v_{esc})^2 - 1]^{1/2}$; a typical Moon-forming giant impact would plot very near the upper left red triangle (45° impact, 1:10 mass ratio, $v_{imp} = v_{esc}$), although satellite formation was not studied here, just computation of $\xi = {}^{M_1 - M}\!/_m$ where M_1 is the total bound mass including any satellite. The plot makes its abrupt transition from efficient accretion to hit-and-run collisions around Safronov number $\Theta < 1$ (see text), for which $v_\infty > v_{esc}/\sqrt{2}$. Other SPH simulations (not plotted) involving targets from Vesta-sized to super-Earth-sized give similar results, in accordance with the expected scale invariance. In the case of perfect mergers, $\xi = 1$ and $M_1 = M + m$. In the limit of no collision $\xi = 0$, $M_1 = M$, and $M_2 = m$. For $v_\infty \gtrsim 0.7\,v_{esc}$ the 45° and 60° impacts – red and green, representing half of all collisions – can perhaps be reasonably approximated as collisionless.

corresponding to the kinds of planetary collisions enumerated above:

1. Effective mergers are the most common occurrence for random velocities $v_\infty \lesssim 0.6 v_{esc}$, corresponding to the cluster of points in the upper left.

2. For the velocity range $0.7 v_{esc} \lesssim v_\infty \lesssim 2.5 v_{esc}$ hit-and-run is the most pronounced outcome, much more common than efficient mergers or disruptive collisions. The clustering around $\xi = 0$ corresponds to impactors "bouncing" from the target with little mass contribution or erosion.

3. Erosive collisions occur for random velocities greater than $\sim 2.5 v_{esc}$. These tend to destroy the smaller body (mos is not accreted) and erode the larger. Accretion is negated, more dramatically as one moves to the right on the plot.

In terms of impact velocity $v_{imp} = \sqrt{v_\infty^2 + v_{esc}^2}$ the range for hit-and-run is $\sim 1.1\, v_{esc} \lesssim v_{imp} \lesssim 2.7\, v_{esc}$. Catastrophic disruption, traditionally defined as $M_1 = M/2$, i.e. $\xi_{cat} = -\frac{1}{2} M/m$, requires collisions at velocities far to the right of this plot.

The most striking part of the plot is the abrupt jump to the hit-and-run line

$$\xi_{hr} \approx 0 \tag{9}$$

at around $v_\infty \sim 0.7 v_{esc}$, marking the transition to collisions where the impactor bouncess from the target. This jump was reproduced by Marcus *et al.* (2009) in their study of impacts involving super-Earth ($1 - 10\, M_\oplus$) scales. Two of the simulations that plot near the hit-and-run line are shown in detail in Figure 7. Because these occur at what are expected to be very typical values of random velocity, considerable diversity is predicted among the styles of planet-forming collisions.

2.6 Prevalence of Hit-and-Run

The prevalence of hit-and-run can be demonstrated in a simple framework model (Figure 8) for hierarchical accretion. The model is not dynamical; planetesimals are given an initial random (but comparable) mass and allowed to grow through randomly selected pairwise collisions. If a colliding pair is within a factor of 30 in relative mass (based on Figure 3) and within a factor of 30 in mass of the largest body (so that $v_{esc} \approx v_\infty$) then it is an SSC and is assigned a random chance ~ 0.3 of efficient accretion (from Figure 6). Efficient accretion is represented as a perfect mass merger, removal of the smaller body, and mass-averaging of the existing hit-and-run tally (which starts off at 0). The corresponding random chance ~ 0.7 is for hit-and-run, which does not change the larger but incrementes the hit-and-run tally of the smaller by 1. Models are also run with $0.5 : 0.5$ probabilities of perfect accretion versus hit-and-run. Pairs with mass ratio $< 1/30$ are always assumed to be perfectly accreted (cratering events). Small colliding pairs, each with masses

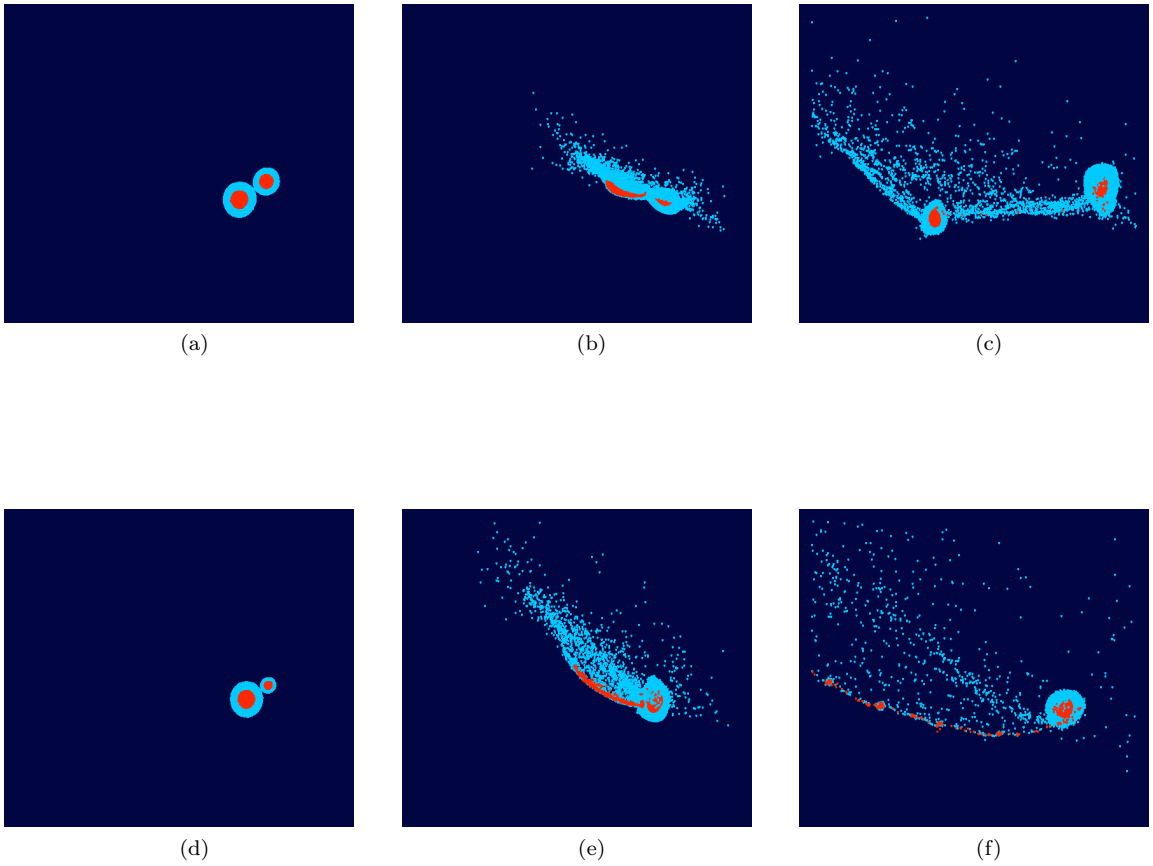

Figure 7: Hit-and-run is a common outcome when planetary bodies of similar size collide. Two collisions are shown from near the hit-and-run line in Figure 6, illustrative of what happens when a large, differentiated body is dashed against a larger target. In this case a Mars-mass planet is struck by a planet half (top) and a tenth (bottom) its mass. Rocky mantle is labeled blue and iron is labeled red; the Tillotson equation of state was used. 3D SPH particles are shown in side view before, during, and 3 hr after the collision. The blue particles appearing to mix into the core are a projection effect of particles with the same (x, y) but different z; for the most part there is little consequence to the core of the target. Planets are in self-gravitational pressure equilibrium, are not rotating, and are launched towards each other at a separation distance $r_o = 5\,R_{roche}$. Impact velocities are modest, $v_{imp} = 1.5\,v_{esc}$ in (a-c) and $v_{imp} = 2\,v_{esc}$ in (d-f). Impact angle is 30° in both cases, which would not count as oblique incidence in impact cratering (see Figure 4). The first scenario results in widespread mantle removal from the impacting planet, which is discussed below in the context of the origin of Mercury. The second case results in a chain of bodies the size of the major asteroids, some quite iron rich and others devoid of core material. [Print in color.]

less than 1/30 the largest, have $v_\infty \gg v_{esc}$ in which case both of the bodies are removed from the population.

Pairwise collisions proceed until the number has been reduced to $N_{final} = 10 - 30$. While there are many possible parameters to play with (initial mass distribution, probability of merger, removal of the smaller bodies) these changes do not affect the basic outcome very much: that hit-and-run occurs numerous times on the way to planet formation, except for those bodies that rapidly accrete to the largest size, so that there is nothing larger to run into. It is not a surprising result; random selection with partial removal rapidly alters the leftovers. In terms of fishing, where one is allowed to keep only the largest fish, by the end of the summer every fish remaining in the lake has had a hook in its mouth several times.

A physical characterization of the process shall require N-body integrations to track actual collisions, and acquiring outcomes directly from Figure 6, or better yet, using direct outcomes from collisional codes since the dynamics change with every impact. But the inescapable result is that hit-and-run occurs commonly to the smaller surviving bodies, and has likely happened several times to most of them. In the case of $N_{init} = 100$ and assuming 50% of impacts resulting in accretion, a few of the largest bodies grow fast enough to avoid the effects of hit-and-run. But any calculation beginning with thousands of bodies ends up with most final bodies having hit-and-run tallies of $\sim 3 - 30$ – a huge amount of material processing and segregation on the way to completed planets, if accretion proceeds under conditions with $\Theta \approx 1$. As mentioned below, much of the stripped material ends up on the largest bodies when all is said and done, so the hit-and-run tallies of the largest may not matter all that much. But in every scenario the unaccreted suffer hit-and-run numerous times.

2.7 The Accreted and the Unaccreted

The above is a shematic study, not a dynamical one. Two bodies that come into close proximity once in their orbits about the Sun, at the relatively low random velocities considered here, are likely to do so again unless their orbits are perturbed. And so, the bodies involved in a hit-and-run collision are expected to come back again to try once more. Given a few tries, accretion is the likely result. This must be the case: Over a few tens of millions of years, it is known from isotopic age dating techniques (e.g. Yin *et al.*, 2002) that accretion won out, and terrestrial planet formation effectively ended in our solar system. The fact that N-body simulations that assume perfect sticking give about the correct accretion timescale, likely implies that perfect merger is not a bad assumption in the sense of correlated encounters: that planets on colliding orbits, for the most part, eventually accrete.

But the bodies that did not accrete onto the largest bodies – the surviving next-largest planets – are not "the most part". They are a fortunate remainder. This review concerns those planets and

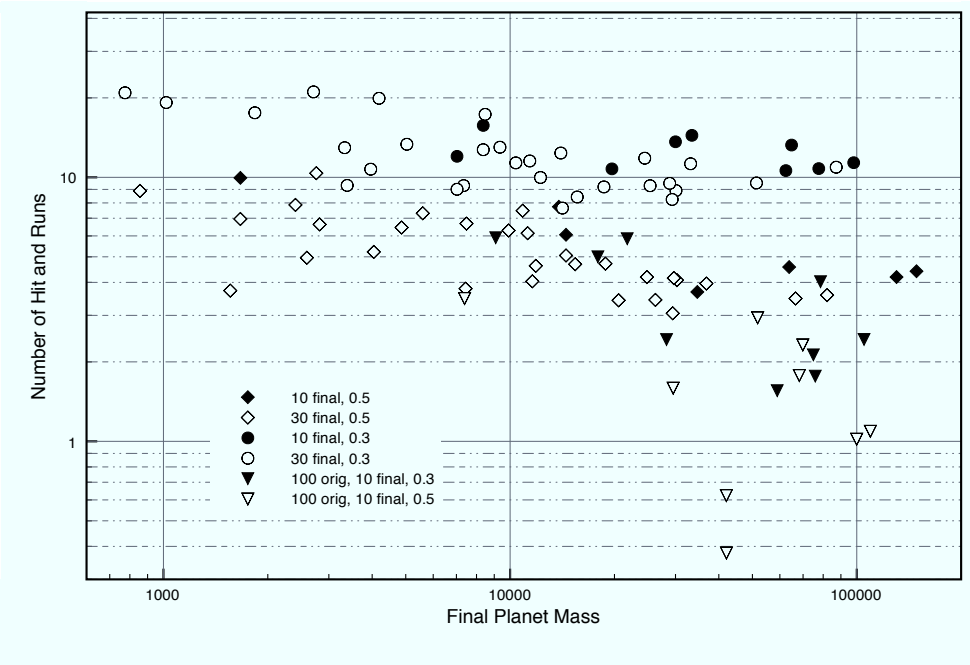

Figure 8: Accretion in the hit and run regime ($0.7\,v_{esc} \lesssim v_\infty \lesssim 2.5\,v_{esc}$; $\Theta \approx 1$) is modeled schematically as a collection of N_{init} planets growing by random pairwise collisions (see text), with hit-and-run, accretion and disruption occurring in approximate concordance with Figure 6. The y-axis shows the number of hit and run events a final body (or its accreted components) experienced by the time a population of N_{init} bodies merges into a final number of bodies (here $N_{final} = 10 - 30$, as labeled). The ratio of accretionary collisions to hit-and run collisions, as labeled, is 0.5 or 0.3, applied at random to each collision. A planet that rapidly grows into one of the largest bodies has nothing larger to collide into. The smallest bodies are assumed to have 100% accretion efficiency with much larger bodies (relatively slow cratering events), but get are assumed to disrupt in pairwise collisions with other small bodies, since $v_\infty \gg v_{esc}$ (see text). For $N_{init} = 10^4$ (circles and diamonds) the final bodies have experienced ~ 10 hit-and-run events; the largest are agglomerations of smaller bodies with past hit-and-run histories. For $N_{init} = 100$ (triangles) there are far fewer collisions required for growth, and a couple of the final bodies have experienced few hit-and-run encounters.

planetesimals that participated in accretion, but by a relatively small chance of dynamics neither merged, nor were scattered, and thus remain behind in the finished population. Planet growth thus proceeds apace for the largest bodies, in the sense that merger usually happens, and because a given hit-and-run collision does not grossly affect the largest target bodies (accretion efficiency $\xi \approx 0$). If it takes several tries, then one can to first order ignore the first unsuccessful attempts at accretion. There is some shock and gravitational evolution, but not much loss or exchange of matter compared to what happens to the bounced-off impactors.

There is, however, a compositional change over time that ends up discriminating the largest from the next-largest planets. With each non-accretionary event the smaller bodies get stripped of their outer layers, become increasingly iron-rich and volatile-poor. If it takes a smaller body several times to accrete, by the time it finally merges its mass contribution will tend to enrich the iron fraction of the target, and not add much in terms of water and atmophiles. The stripped oceans, atmospheres, crusts and upper mantles of hit-and-run survivors go back into the disk; discrete parcels of stripped material will have dynamical parameters that make future encounters with the colliding pair of planets likely. Being much smaller than R and r, future impacts by these parcels with either of the colliding pair will be cratering events (not SSCs) and thus likely to result in accretion. The material is much more likely to be accreted by the object with the larger cross-section; gravitational focusing makes the probability $> (R/r)^2$ that it will reaccrete onto the largest of the colliding pair. The largest bodies are thus expected to rob, over time, the exterior materials from the next-largest bodies, leading to a compositional dichotomy between the accreted and the unaccreted.

3 Departures from Scale Invariance

The above simulations are based on fully compressible fluid dynamics computations including the calculation of shocks and the reasonably accurate calculation of the equation of state relations $P(\rho, u)$ where P is pressure and ρ, u are density and internal energy of the represented material. Simulations using the same SPH code and Tillotson EOS indicate scale invariance for equivalent impacts involving planets ranging from Vesta-sized to Earth-sized, when the velocities are scaled to v_{esc} and when the planets have the same differentiated 30/70 wt% iron/silicate composition. Using a different SPH code and EOS model (and minor differences in setup) Marcus *et al.* (2009) reproduce part of Figure 6 for super-Earth-sized planets and obtain very similar results at a larger scale.

But similarity in computational results is not proof of scale invariance in nature! The complexities of geology not included in these simulations can perhaps be reduced to key approximations to geophysical behavior, especially brittle and viscous rheology and the physics of dynamical magmatic systems. In addition one must understand that impact physics itself changes fundamentally as one transitions from hypersonic events (much faster than the sound speed in the rock) to sub-

sonic events, the transition being a few km/s for rocky bodies but much slower for uncompacted bodies. Along these lines, one can identify four primary reasons to expect departures from scale invariance as one transitions from large, differentiated, molten planets, to SSCs involing smaller colliding pairs:

Rheology. Brittle mechanical strength is size and rate variant (Grady and Kipp, 1985; Melosh *et al.*, 1992). Strength itself is poorly understood at medium-range velocities (tens of m/s) that may be common among growing planetesimals. As for deformation on the timescale τ_{grav} of a similar sized collision, large bodies are likely to be dominated by viscous rather than brittle deformation, first because they are massive – their deep pressures far exceed the energies associated with the failure of elastic solids – and because they retain more heat. The viscous strain rate $\dot{\epsilon} = \sigma/\eta$ times the encounter time $\tau_{coll} \approx \tau_{grav}$ must exceed a factor of several, for disruption to occur, where σ is approximately the gravitational stress $\sim G\rho^2 r^2$, allowing for η_{max} to be computed for the limit of disruption.

Differentiation. Closely related to the thermal state, or past thermal state, is the transition with increasing size towards differentiated internal structures with greater binding energy. Colliding bodies whose iron has segregated to the center, and whose atmosphere and volatile condensates (oceans) have migrated to the exterior, behave differently than undifferentiated colliding spheres, sheltering their cores and leading to the preferential removal of lower-density outer materials that are at low gravitational potential and receive the brunt of the impact energy. Impedence mismatch at the core-mantle boundary (Asphaug, 1997) may also enhance the velocity of ejected materials from the outer layers. These effects change the physics with scale, and work to segregate planetary materials.

Shocks. Because impact velocity of SSCs scales approximately with the size of the colliding bodies ($v_\infty \approx v_{esc}$) there is a tendency for large enough impacts to produce shocks, at impact velocities far exceeding the sound speed of their material. For giant impacts at tens of km/s, shocks can induce global melting, while for primary-accretion collisions at a few m/s the impacts are subsonic and may only result in damage (if solid) or in compaction or shear bulking (if granular; see e.g. Schäfer *et al.*, 2007). Shocks are less important at more grazing incidence.

Unloading. The lithostatic overburden pressure of a non-rotating incompressible planet of radius r is $P(a) = {}^2/_3\pi G\rho^2(r^2 - a^2)$ where a is the distance from the center. The characteristic pressure $P_o = G\rho^2 r^2$ is released to a much lower value during the collision timescale τ_{coll}. The effect of ΔP can be subtle for small bodies – it may have been expressed in the vigorous dust production of comet Shoemaker-Levy 9 after its tidal disruption by Jupiter (Hahn and Rettig, 2000) – and it can be hugely important for larger bodies. If one thinks of planetary

disruption as an enthalpy-conserving event, and ignores shocks, then the change in specific enthalpy goes as r^2. For bodies that are Moon-sized and larger, there is enormous potential for widespread eruptive degassing and hydrothermal action at global scales, even in response to purely tidal (beyond-grazing) collisions. Based on Earth analogues, pressure release melting and plinian-type magmatic responses are expected, occurring at global scales.

3.1 Rheology

Rheology pertains to how geological materials deform and flow. In the simplest application, rheology can be thought of as a strength (that is, a yield stress) beyond which material flows, for instance as a viscous fluid. Strength itself is quite complicated, but we take a simple approach.

Strength

Strength is scale variant because small objects have smaller flaws. If one thinks of an object's volume as sampling a probability distribution of possible flaws (Weibull, 1939; Grady and Kipp, 1985) then static tensile strength, expressed as the weakest flaw present in a volume, decreases approximately with size to a power $r^{-3/m}$ where $m \approx 6 - 9$ for typical igneous rocks. This leads to the fact that large asteroids require less energy to catastrophically fragment than small ones, whether by tides or by collisional stresses – fragment, that is, but not disrupt. Large asteroids are more tightly bound gravitationally and more difficult to disrupt. The simple corollary is that rubble piles – gravitationally bound piles of fragmental debris – are ubiquitous for asteroids larger than about 300 m diameter (e.g. Benz and Asphaug, 1999) but only up to the point that self-gravity and internal heating compactifies the planet into a coherent body, and its overburden shields it from tensile stress.

Cohesion in the context of tidal disruption was first explored by Jeffreys (1947) in his analysis of the gravitational disruption of planetesimals passing inside the Roche limit of Earth. He found that a monolithic asteroid smaller than a few 100 km diameter will survive grazing passage near the Earth, and that a larger asteroid will be disrupted. This conclusion was derived by equating the maximal tidal stress (which increases with the square of impactor size) against tensile strength, which Jeffreys assumed was not size-varying.

As with most pioneering research, the result was eventually rendered somewhat moot (tensile strength is not really applicable to rubble piles) yet provides lasting insight. The smallest asteroids might be structurally intact (monolithic) in which case they do not come apart by tides. Indeed, there is evidence from the imprint of tidally disrupted comets upon Jupiter's satellites – or specifically, the absence of the imprint of tidally disrupted comets smaller than about 100 m – that small Jupiter-family comets might be structurally competent (Asphaug and Benz, 1996). But structural competency is relative to the tidal stress, which across such a small body is not much greater than

that of a dry snowball. For SSCs, tidal stress scales as the pre-impact hydrostatic stress.

We have witnessed tidal disruption in modern times, by comets coming close to Jupiter and the Sun. Comet Shoemaker-Levy 9 was a 2 km diameter body of density about 0.6 g cm^{-3} (Asphaug and Benz, 1994) that encountered Jupiter in 1992. It came apart much as a liquid body would, over the course of the few hours it spent inside the Roche limit of Jupiter. The evidence of crater chains on the Galilean satellites of Jupiter strongly suggests that all comets that are tidally disrupted by Jupiter do so as strengthless, fluidized rubble piles (Asphaug and Benz, 1996; Schenk *et al.*, 1996).

If comets (and perhaps by extension small rubble-pile planetesimals) behave as self-gravitating fluids during gravity-dominated planetary encounters, then perhaps there is similarity of SSCs even to the scales of small planetesimals during the earliest epochs of planet formation when impact velocities were slow. Detailed numerical models (Schäfer *et al.*, 2007) and laboratory experiments (Wurm and Blum, 2006; Dominik *et al.*, 2007) of colliding porous aggregates give various results, but all show how crushable or fractal solids can behave in unexpected ways. It is difficult to guess, but strength may play a major role in similar sized collisions up to 100's of km diameter, which is also to say, for v_{imp} of a few times $v_{esc} \sim 0.1 - 1$ km/s.

While on the topic of strength, it is worth noting that ejection velocity from a rocky target scales approximately with the square root of tensile strength, since strength is a specific energy $\sim v^2$. Thus, the strength of rock strongly biases which meteorites we look at, by sending the strong ones on the quickest journeys to Earth, where in turn they are most likely to survive atmospheric entry and terrestrial residence prior to discovery and curation. Warren (1994) notes that lunar meteorites, ejected at hypervelocity from the Moon, are much harder to crush for laboratory analyses than rocks selected from the surface by Apollo astronauts. Head *et al.* (2002) and Bart and Melosh (in press) find enhanced ejection velocities in competent materials in accordance with theoretical expectations.

Viscosity

If colliding planets are large enough, or molten, then strength and cohesion are of no concern, and the principal sources of scale invariance are the density, the equation of state, and the deformation rheology. Regarding the latter, one approach is to consider a linear (Newtonian) viscosity limiting the rate of strain.

If a fluid planet's viscosity resists deformational shears on the collision timescale, then disruption will not occur. Viscosity is the ratio of the stress to the strain rate,

$$\eta = \sigma / \dot{\epsilon} \tag{10}$$

A similar sized collision takes place over the gravitational timescale $\tau_{grav} = \sqrt{3\pi / G\rho}$, a couple of hours for density corresponding to terrestrial planet-forming materials. The strain rate of

deformation is then

$$\dot{\epsilon} = \epsilon/\tau_{grav} \tag{11}$$

for some shear strain ϵ. If the stress is primarily gravitational (as would be the case for tidal or shear disruption against self-gravity) then the characteristic stress is

$$\sigma \sim P_o \sim G\rho^2 r^2 \tag{12}$$

where r is the radius of the disrupted body.

The smallest impactor r_{min} that can come apart in an SSC is therefore

$$r_{min}^2 = \eta\epsilon/\sqrt{3\pi G\rho^3} \tag{13}$$

in the sense that the required deformation rate $\dot{\epsilon} = \epsilon/\tau_{grav}$ is accommodated by the viscosity η. This expression is plotted for various values of global strain ϵ in Figure 9, for planets of bulk density $\rho \sim 4$ g cm^{-3}. Strains of 1, 10, and 100 are plotted – a wide enough spread to bracket catastrophic disruption. Strain $\epsilon \gtrsim 10$ occurs for

$$\eta \lesssim 10^{13}(r/1000\,\mathrm{km})^2 \tag{14}$$

where units are poise (g cm^{-1}s^{-1}). Walzer *et al.* (2004)adopt mid-mantle viscosities $\sim 10^9$ poise in models of early Earth convection, and Tackley (2001) uses $\eta \sim 10^9 - 10^{13}$ poise in Io asthenosphere models. Moon-sized planets that have bulk viscosity corresponding to a partial melt ($\eta \simeq 10^{14}$ poise) will certainly behave as fluid bodies in an SSC encounter, as will impactors as small as 10 km that are fully molten ($\eta \ll 10^8$ poise).

To obtain a simple rule of thumb, let a characteristic strain $\epsilon \approx \sqrt{3\pi}$ correspond to disruption; then the maximum viscosity that allows for the disruption of a planet of radius r is

$$\eta_{max} \approx r^2\sqrt{G\rho^3} \tag{15}$$

Because this maximum allowable viscosity increases as r^2, while the planet's viscosity deacreases with r due to internal heat retention, the transition from viscous-limited to inviscid behavior is

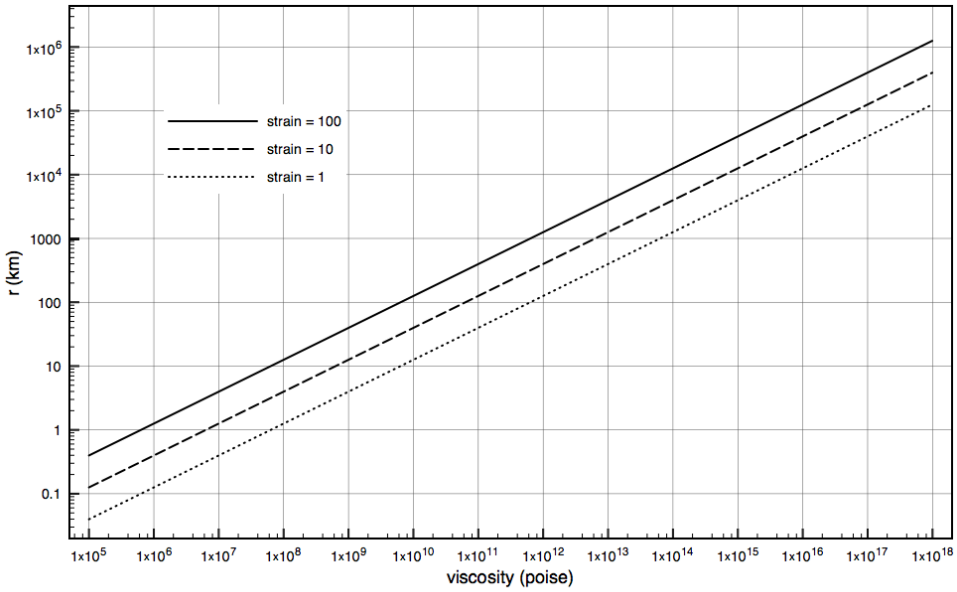

Figure 9: These lines plot the minimum radius r_{min} of planet that can deform to a total strain $\epsilon = 1$, 10, 100 during a gravity-dominated similar-sized collision (see text). The onset of significant prolate deformation is marked by $\epsilon = 1$, while $\epsilon \sim 10$ is disruptive and $\epsilon = 100$ catastrophically disruptive. Terrestrial planetary density $\rho = 4$ g cm^{-3} is assumed. The calculation is an upper limit to the threshold size r_{min}, since viscosity is reduced by stress-dependent effects and by impact shocks and pressure release melting.

likely to be abrupt, represented by a cooling curve that would plot from upper left to lower right in Figure 9. If so, then planets transition in collisional behavior as they increase in size, with SSCs smaller than r_{min} resisting deformation and those larger than r_{min} behaving as inviscid gravitating fluids. Because temperature T is a sensitive function of r, the transition may be abrupt as an early planet grows.

Four effects make the response to similar-sized collisions more fluid (less viscous) than plotted in Figure 9. First is the fact that rocks, partial melts and magmas are nonlinear fluids, whose effective linear viscosity decreases with a power of the stress. This means that viscosity $\eta \sim \sigma/\dot{\epsilon}$ is much lower for larger-scale collisions because overburden stress P_o is larger by r^2. Second, pressure release melting acts to lower the viscosity during a collision, of significance for partially molten or larger planets. Third, the exolution of volatiles during pressure unloading can initially act to increase the viscosity of a magma by stiffening it with bubbles, but at high enough deformation rates and degassing rates the low viscosity of the gas wins out, and bulk viscosity plummets (see e.g. Gardner *et al.*, 1999; Alidibirov and Dingwell, 1996). And lastly, any shocks or damaging stress

waves accompanying the collision further act to fluidize the planet (Asphaug and Melosh, 1993). All in all, it appears that similar sized collisions larger than a few 100 km in scale, and perhaps as small as ~ 10 km if internally heated by active ^{26}Al, are inviscid and deformable as modeled.

3.2 Differentiation

Viscosity's exponential dependence on $1/T$ leads naturally to a consideration for the heat sources availale in planets before, during, and after a similar-sized collision, and to the behavior of differentiated (melted) bodies versus undifferentiated bodies.

During the primary phases of planetesimal formation, thermal energy is available from many sources, including impact shocks (from turbulence or infall), nebular shocks, solar heating, and the decay of short-lived radionuclides (see for instance Wasserburg and Papanastassiou, 1982). Regarding solar heating, the radiative equilibrium temperature at the present-day orbit of Mercury is not hot enough to melt rock, only ~700 K at best, although burts of intense heating from an early sun wouls lead to some silicate melting in the innermost disk. But it is not believed to be volumetrically important for terrestrial planet formation. Nebular heating by shocks can be very intense, and is proposed (Desch and Connolly, 2002) to be responsible for the melting of chondrules. While this heat source was likely to be prevalent and intense, it diminishes rapidly once planetesimals accrete, due to the clearing out of the gas and dust which carries the shocks. As for impact shock heating, driven by gravitational particle scattering and turbulent entrainment, this is certainly a significant heat source during collisions in the late stage of giant impacts, although not early on when collisions are slow. Even when hypervelocity impacts into small bodies do occur, as in the present solar system, they do not contribute to the bulk melting of small bodies, as melt products are shock-accelerated and mostly escape from an asteroid's low gravity. Melting of small bodies requires something else.

It is now generally acknowledged that the most important heat source for thermal processing during primary accretion was, in our solar system, the decay of $^{26}\mathrm{Al} \rightarrow ^{26}\mathrm{Mg}$, a radionuclide with half life $\tau_{1/2} = 7.2 \times 10^5$ yr (Bizzarro *et al.*, 2005). While the origin of ^{26}Al is much debated, its original abundance in our solar system is measurable in meteorites. For chondrites the initial $^{26}\mathrm{Al}/^{27}\mathrm{Al} \simeq 5 \times 10^{-6}$, whose decay over $\tau_{1/2}$ releases several times more heat (in erg g^{-1}) than required to bring cold, dry dust to the melting point. Other short-lived radionuclides, notably ^{60}Fe, were trapped in early-forming rocks in our solar system, also long-spent but evidenced by their daughter products; their heat production is not believed to be as significant as ^{26}Al in our own solar system.

The prevalence of ^{26}Al in other solar systems is unknown; this is a critical piece of missing knowledge since its presence or absence has the potential to dramatically alter the mechanism of primary accretion. A solar system with, say 10% of our measured ^{26}Al might not produce enough

heat for its early small bodies to melt. If small planetesimals remain unmelted, even as they grow larger than ~100 km, then the character of their impact coagulation might change, conceivably even shifting the growth of planets away from the terrestrial planet-forming region, or biasing the favored size of finished planets. Astrobiologically ^{26}Al could be a matter of life or death.

The rate of heat production $\mathrm{d}q/\mathrm{d}t$ in a planet from radionuclide decay is proportional to the mass $\sim {}^4\!/_3\,\pi r^3\rho$. Thermal energy dissipates by conducting through the solid and radiating from the planet's surface area $\sim 4\pi r^2$ at a temperature T, per unit area with a blackbody flux σT^4. The heat produced, divided by heat radiated, goes as r, and increases greatly with temperature. Large planets thus attain radiative equilibrium at higher temperature and get hot enough to melt. According to 1D thermal modeling by Merk *et al.* (2002), a 10 km diameter homogeneous chondritic body accreting much faster than $\tau_{1/2}$ easily melts; see Ghosh *et al.* (2006).

Timing is everything, and so is location: planetesimals forming closer to the Sun acquire a greater fraction of Al-bearing silicates than those forming where ices dominate; they also accrete much more rapidly. They are thus much more prone to melting than bodies forming much further out. The transition from fluid to solid behavior, plotted in Figure 9 in terms of planetary radius, might also be an abrupt transition in time: the half-life of ^{26}Al is – interestingly enough – comparable to the timescale of primary accretion, and therefore it is certainly likely that this energy source would run its course through several half-lives as a planet grows.

3.3 Energy of Collision

Catastrophic disruption is defined as leaving a target body with no more than half of its original mass either intact or gravitationally bound; in terms of Figure 6 ξ is a large negative number to the lower right of the data, $\xi < -\frac{1}{2}\frac{M}{m}$ and $v_\infty \gg v_{esc}$. This is a relatively common impacts for collisions into small asteroids and comets in the present solar system, in which case catastrophic disruption is achieved by relatively small projectiles $m \ll M$, so that catastrophic disruption can be modeled (as with impact cratering) as a point-source event.

In the target-centric view of things, the characteristic threshold of catastrophic disruption is traditionally expressed in terms of the specific impact kinetic energy ${}^1\!/_2\,mv_{imp}^2$ per unit target mass M:

$$Q = \frac{1}{2}mv_{imp}^2/M \tag{16}$$

where the disruption threshold Q^* is the value of Q at which the final largest remnant $M_1 = M/2$. For SSCs where $m \sim M$ the specific energy of impact must be defined as $Q = {}^1\!/_2\,mv_{imp}^2/(M+m)$. One might then by analogy want to define Q^* as forming a largest remnant with half the combined

mass, $M_1 = (M + m)/2$. This is readily seen to be inadequate for SSCs, since two just-grazing, equal-mass planets would each have half the total mass for any impact velocity. We must think of disruption in terms of the fates of both bodies.

The smaller body in a colliding pair always suffers the greatest harm, and this is what makes hit-and-run collisions so transformative for the next-largest bodies in an accreting terrestrial planetary system. The tidal stress on the smaller by the larger, compared with the tidal stress on the larger by the smaller, is of greater magnitude in the smaller body in inverse proportion to its mass. In the case of direct collisions, the contact stress wave or shock wave is generated symmetrically about the contact front of a colliding pair, so that energy is partitioned equally into both bodies, so that energy density is inversely proportion to mass. As for the impact differential stress, this can be thought of as the differential deceleration across the diameter of each colliding body, for instance in an off-axis SSC where ˜half of the colliding mass is abruptly decelerated and half is not. If the contact forces are symmetric, then the smaller body decelerates more abruptly than the larger in inverse proportion to its mass. And so, as a rule of thumb, when planets of sizes $r \lesssim R$ collide, then the specific tidal, gravitational, shear and shock stresses felt by each body scale inversely to the mass ratio m/M. In the case of the Moon-forming simulation of Figure 5, the impactor, being an order of magnitude less massive than the target, suffered an order of magnitude greater damage, expressed as the gravitational, mechanical and shock energy of collision per unit mass.

Whether shocks, tides or shears dominate and impactor's disruption is a function of geometry, from just-grazing (where tides dominate) to head-on (where impact stresses and shocks dominate). In SSCs the impact kinetic energy per unit mass $\sim v_{imp}^2 \sim v_{esc}^2 \sim GM/R \sim R^2$, partitioned as above between the impactor and the target. In an isolated planetesimal swarm with no bodies larger than $\sim$ 1000 km, random speeds are generally subsonic. But once Moon-sized planets exist, stirring the swarm to km/s velocities, the shock effects of impacts can become significant.

3.4 Enthalpy of Unloading

The total gravitational binding energy of a uniform planet of mass M and radius R is

$$U_B = \frac{3}{5} GM^2/R \tag{17}$$

which, like accretional impact energy, scales $\sim R^2$ per unit mass. Binding energy U_B is the energy required to disassemble a planet gently to infinity, and thus represents the lower limit of the kinetic energy $\sim \frac{1}{2} v_{esc}^2 dm$ of all masses dm that contributed to the formation of the planet from $v_\infty = 0$, with v_{esc} increasing as the planet grows.

The total kinetic energy of impacts is several times the binding energy for typically stirred up

populations, going as $1 + {}^1/_{2\Theta}$. This energy dissipates (through shock and frictional effects) as a significant amount of heat for a large enough body. For a planet the size of Mars, the gravitational binding energy is $\sim 5 \times 10^{37}$ ergs. Assuming Safronov number $\Theta \approx 1$ the energy of impacts was of order 10^{38} ergs. Divided by the heat capacity for rock ($c_p \approx 8 \times 10^6$ erg g^{-1} K^{-1}) and the mass of Mars (6.4×10^{26} g) this gives an estimate for its heating due to impacts: of order 20,000 K (telling us that constant heat capacity is not an adequate assumption). For a Vesta-sized planet, the same calculation gives a heating of about $\sim$ 100 K. Owing to the R^2 dependence, for smaller asteroids accretional heating is especially insignificant.

Of course, Mars-sized planets never get that hot; they radiate to space. But some of the accretional energy is stored as internal energy u, and some is stored as enthalpy of compression, solution, and phase change. The specific enthalpy of a planetary interior is

$$h = u + P/\rho \tag{18}$$

where P/ρ is the pressure times the specific volume $V = 1/\rho$. Changes in enthalpy which can drive reactions are thus

$$dh = du + PdV + VdP \tag{19}$$

It is very useful to think of SSCs in terms of enthalpy for the same reasons that enthalpy is the guiding state variable for the modeling of rising magmatic conduits (e.g. Wilson and Keil, 1991). During large-scale similar sized collisions, the drop in pressure VdP as the planet comes apart leads to an abrupt change dh over the timescale τ_{grav}, and this can drive various reactions forward.

Huge specific enthalpy is made available in the aftermath of Vesta- to Mars-sized SSCs. Hydrostatic pressure P increases with more than the square of a planet's radius, since rocks are compressible. Because the timescale of collision is invariant in SSCs, both the total pressure release ΔP and the rate of pressure release dP/dt scale greater than R^2. The high magnitude and rate of unloading during disruption can drive cavitation, the dissolution of volatiles, bubble nucleation and coalescence, magmatic forcing, and pressure release melting.

This causes us to look at the volcanic eruption modeling of Gardner *et al.* (1999) and others. The pressure drops and their timescales, for Vesta- to Mars-sized SSCs, are comparable to strombolian-type eruptions, which are driven by gas bubbles rising faster than the surrounding melt. Recent measurements at Stromboli volcano (Burton *et al.*, 2009) show gas slugs originating at ~3 km depth in Italy, on Earth. These same pressures are attained in the middle of a 500 km diameter planet. One might surmise that strombolian eruption physics might drive the degassing of large molten planetasimals in the aftermath of hit-and-run collisions, and their magmatic fragmentation

(Alidibirov and Dingwell, 1996).

As pressure is released, uncompensated pressure gradients result in accelerations that can change the dynamics of disruption, possibly contributing to the shedding of material or the emplacement of a debris disk. Pressure gradients played a role in the formation of the protolunar disk (Stevenson, 1987), and the disk formed not only from material released from impact shock pressure, but also from material that released from a high pre-impact hydrostatic state P_o. Most of the disk-forming material in the Moon-forming simulations (e.g. Figure 5) emerges in the course of a few hours from several tens of kilobars of pressure.

Tidal Collisions

The best way to appreciate the physics of unloading is to isolate it, in a purely tidal collision. In a tidal collision $b \gtrsim r+R$, so that the smaller planet is well inside the Roche limit of the larger planet, $R_{roche} = 2.423R(\rho_R/\rho_r)^{1/3}$. This is the distance from a planet of radius R, density ρ_R where an incompressible small fluid spheroid ($r,\ \rho_r$) on circular orbit will be disrupted (Roche, 1850). The Roche limit is not directly applicable to parabolic or hyperbolic encounters (see for example Sridhar and Tremaine, 1992); tidal disruption of the smaller body along a near-miss requires a closer encounter. For small strengthless incompressible bodies encountering massive planets at $v_\infty = 0$, Asphaug and Benz (1996) found that periapse inside $\sim 0.69\, R_{roche}$ is the threshold for the shedding of matter, in agreement with the analytical result of Sridhar and Tremaine, and that passage inside of $\sim 0.55\, R_{roche}$ results in the loss of half the mass, stripped from the exterior.

Things are of course different during similar-sized tidal collisions because $r \sim R$. The impactor is extensive, and part of it will be on collision course when $b \approx r + R$. But as a benchmark, if $\rho_R = \rho_r$, then $0.5\, R_{roche} \simeq 1.2\, R$, so that to first order we expect catastrophic tidal disruption when a planet $r \lesssim 0.2\, R$ is on grazing parabolic incidence. Figure 10 summarizes purely tidal encounters (from in the context of small spherical bodies of density 0.6 g cm^{-3} ("comets") and 3 g cm^{-3} ("asteroids") encountering planets of various density. As can be seen in this figure, in the limit of $r \ll R$ a catastrophically disruptive tidal collision is about half as likely, between an asteroid and Earth, as a physical collision; for comets tidal disruption is $\sim 3/2$ as likely. For equal density bodies on parabolic encounters with $r \ll R$, catastrophic tidal disruption is $\sim 1/3$ as likely as collision.

For studying compressible, differentiated planets undergoing tidal collisions, SPH is one of the best tools. Figure Below shows the result of a simulation (Asphaug *et al.*, 2006) in which a Moon-size ($0.01M_\oplus$) differentiated terrestrial impactor, with composition 70 wt% rocky mantle and 30 wt% iron core as in all other simulations, and the same Tillotson equation of state, encounters a Mars-size ($0.1M_\oplus$) impactor. The impactor is initially a non-rotating, isostatically equilibrated sphere. There is no physical contact, only gravitation and pressure unloading, so that the target planet (represented by the open red circle) has been represented in the simulation an undeformable sphere centered on the red dot. The closest-approach velocity is $1.05\, v_{esc}$ and the closest approach

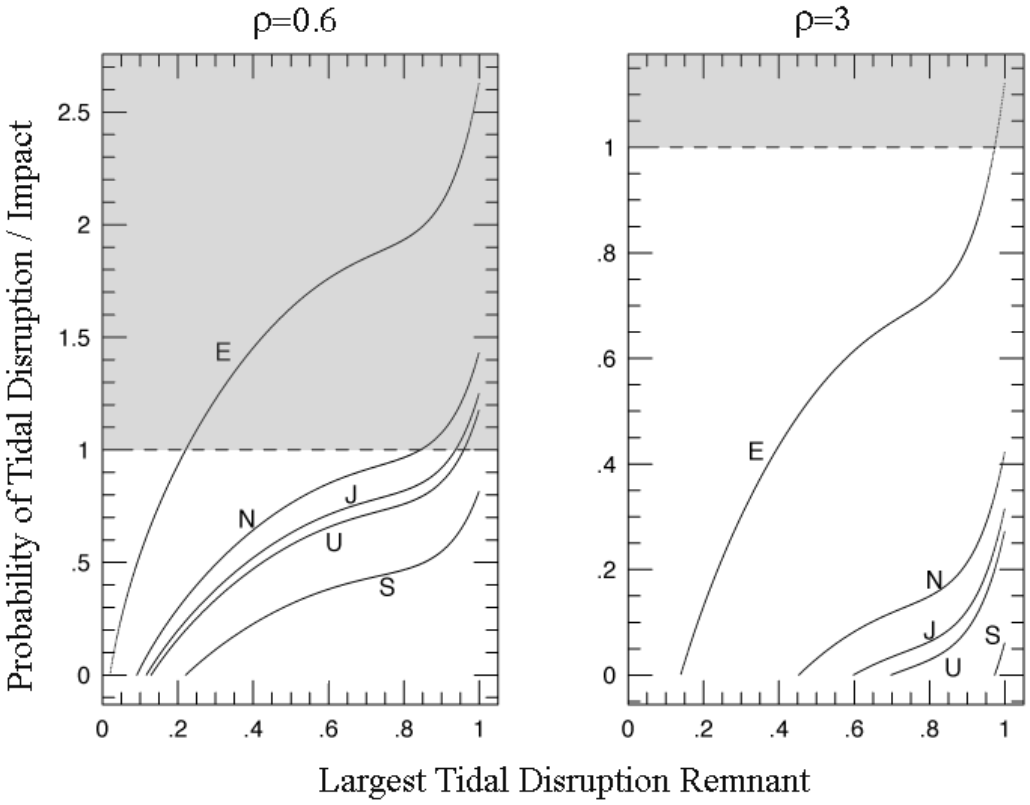

Figure 10: Tidal disruption of small incompressible spheres of density $\rho_c = 0.6$ g cm^{-3} ("comets", left) and $\rho_a = 3$ g cm^{-3} ("asteroids", right) during parabolic ($v_\infty = 0$) encounters with planets in our solar system: $\rho = 5.52$ g cm^{-3} (Earth), 1.66 (Neptune), 1.31 (Jupiter), 1.19 (Uranus), and 0.69 (Saturn), fitted to suites of simulations (Asphaug and Benz, 1996). The probability of a tidal event with a given level of disruption (M_2/m between 0 and 1, in the previous discussion), is plotted normalized to the probability of a physical collision. For example, the disruption of comet Shoemaker-Levy 9 was supercatastrophic ($M_2/m \approx 0.2$) with periapse $1.31\,R$. A tidal encounter this close or closer, but not impacting, is 0.2 times as likely as impact with Jupiter. Asteroids are catastrophically disrupted ($M_2/m = 0.5$) by tides near terrestrial planets $\sim 1/2$ as often as they collide; comets are catastrophically disrupted by tides near terrestrial planets $\sim 3/2$ as often as they collide.

distance is $b = 1.05(R + r)$. The two planets are represented in the center of mass frame, so that the larger is displaced towards the top of the figure in each time step, while the smaller swings from the right towards the bottom and is severely deformed and stripped. The result of this purely gravitational encounter is mass loss, spin-up, and global pressure unloading.

The pressure drop for this tidal collision is plotted below, in terms of pressure inside the Moon-sized impactor, normalized to the initial central pressure $P_c = {}^2/_3 \pi G \rho_r^2 r^2$, measured at the center of the planet (black) and at the core-mantle boundary (grey). Pressure unloading begins about half an hour before periapse, as the larger planet's tidal field competes with the smaller planet's self-gravitational field, and reaches a maximum of $40 - 50\%$ about half an hour after the event. Notice that the unloading at the center takes slightly longer to complete as the signal from surface mass removal propagates inward. The greatest unloading goes on for an hour after periapse; permanent unloading by $\sim 20\%$ in the aftermath is due to spin-up (the final body is rotating with a period ~ 6 hrs) and mass loss.

In hyperbolic ($v_\infty > 0$) tidal collisions with the same periapse $b > r + R$, the chief change is for the unloading to be of shorter duration. In a hit-and-run collision with $b < r + R$, pressure unloading is even greater, as the periapse is closer, but shock and collisional shearing play an increasing significant role as the fraction of intersected mass f increases. For disruptive hit-and-run collisions such as Figure 7d-f, the final pressure unloading in the disrupted fragments approaches 100%, after all is said and done, as the material is now found in bodies with much smaller radii than before. In this case of Figure 7f, the pressure drop experienced by material in the largest remnant is $\sim 90\%$.

4 Discussion

The minor planets in our solar system are incredibly diverse, owing to the fact that they are pieces of differentiated planets that were torn asunder in a process that enhances material segregation on the basis of density; that liberates volatiles from depth; that makes available considerable enthalpy that can drive reactions and eruptions forward; and that can shear apart differentiated parent planets into smaller children planets, each with a new bulk chemistry and volatile, rock and iron fraction, and its own cooling history.

4.1 Roaming planets

The severe and global-altering collisions depicted in Figure 7 are proposed to have happened to a significant fraction of the largest bodies in the present Main Belt, and to perhaps half (that is, Mercury but not Mars) of the minor terrestrial planets in the terrestrial planetary region. The statistics of large numbers (Figure 8) makes this conclusion robust for the minor planets of the

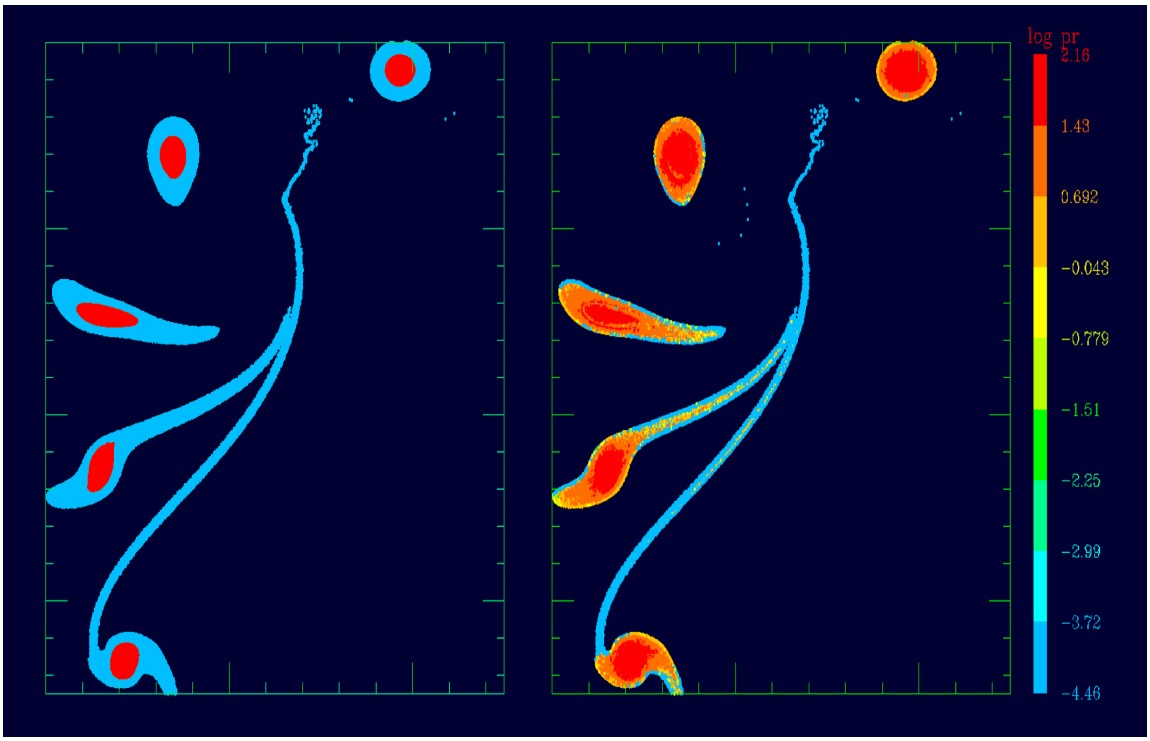

Figure 11: Tidal collision with closest approach velocity $v_{imp} = 1.05\, v_{esc}$ and closest approach distance $b = 1.05(R + r)$, just beyond grazing, corresponding to Figure 12 below. The impactor is Moon-size ($0.01 M_\oplus$). The target is a Mars-size ($0.1 M_\oplus$) body, represented as an undeformable sphere which erases intersecting impactor particles (to minimize collisional interaction in this end member case; a few stray particles result). The simulation begins with a hydrostatic, nonrotating impactor at $5\, R_{roche}$ from the target planet, and well to the upper right; the snapshots are one per hour for five hours around the periapse. The left plot shows the matter (blue rock over iron core), here as a slice through the symmetry plane. To the right are the corresponding pressures, in log code units, where orange $\sim 10^{11}$ dyn cm^{-2} and blue $\sim 10^{7}$ dyn cm^{-2}. Tidal stresses and the shedding of matter and rotational stresses result in greatly rreduced pressure, and greatly increased pressure gradients. [Print in color.]

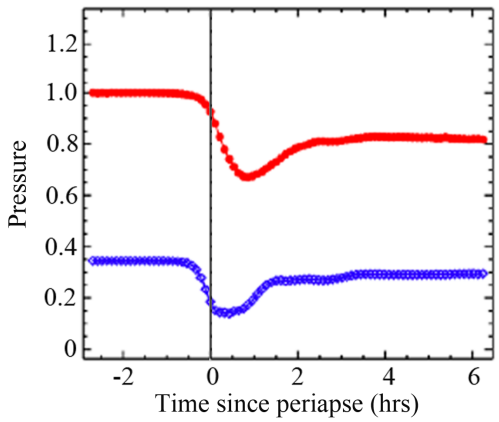

Figure 12: Pressure unloading plot corresponding to the encounter in Figure 6. Vertical axis is the pressure, divided by the central pressure of the planet. Measured pressures are plotted over time at the planet's center (black) and averaged over the core-mantle boundary region (grey). Time is measured in hours before and after the periapse. Global pressure unloading by up to $40 - 50\%$ begins about half hour before periapse, due to tidal unloading, and continues for an hour after. Global pressure is unloaded permanently by 20% in the aftermath due to spin-up (the final body is rotating with a period 6 hrs) and mass loss. Adapted from Asphaug et al. (2006). Print in greyscale.

Main Belt, where it seems rather certain that larger bodies once roamed. For Mercury and Mars it depends upon the late stage dynamics – whether these next-largest bodies had any larger planets to run into, by the time they were close to finished forming.

Earth finished its accretion by mopping up dozens of Ceres- to Mars-sized bodies, becoming an amalgam of numerous smaller feeding zones (e.g. Chambers and Wetherill, 1998). One of these giant impacts formed the Moon, which in a sense is the archetypal unaccreted body. That is to say, the Moon is the unaccreted (but gravitationally bound) remnant of a highly selective process we call, as a whole, accretion, but which in fact is an ensemble of parallel processes that can be seen in Figure 6 to consist, in about equal measure, of mass mergers and hit-and-run collisions, for the kinds of sizes and velocities believed to dominate this epoch (Agnor *et al.*, 1999).

George Wetherill, among the first scientific advocates of late stage cataclysmic collisions, conducted Monte Carlo integrations of planet accumulation and found that planets the size of the Moon and Mars may well have roamed the Main Belt for a few tens of Ma. Wetherill (1992) determined that Mercury could have been born beyond Mars and worked its way in, a result of further consequent interest below. His early results were subsequently confirmed using discrete N-body methods Chambers and Wetherill (1998, 2001); Petit *et al.* (2001).

Chambers (2007) postulated that a Mars-mass body might have survived beyond the Main Belt for hundreds of millions of years, until it became decoupled by a chaotic interaction. During this time many Psyche- to Ceres-sized (say, up to 1000 km diameter) interlopers would have encountered the bodies that were several times larger (up to Mars-sized). About half the time – more often if the random velocities are slow ($\Theta > 1$), less often if they are fast, as per Figure 6 – these bodies would have added their mass to these growing (now lost) planets in efficient merger. About an equal fraction (or greater, for expected values of Θ) they would have bounced off in hit-and-run collisions.

In the outer solar system, where chaos during giant planet migration is believe to have scattered up to 10 Earth-masses of icy bodies beyond Neptune, of which perhaps 0.1 $M_\oplus$ remains ((Levison and Morbidelli, 2003), the scenario is not much different. Among the differentiated bodies of the outer solar system, a number are expected to be stripped by hit-and-run collisions just as has been proposed (Asphaug *et al.*, 2006) for the Main Belt. For example, a Pluto-like body with a rocky central core and icy mantle has a certain probability of having its mantle stripped, resulting in an outer solar system body of mostly silicate composition. The density ratio of rock:ice is greater than that of iron:rock, and thus if all else is equal the process may be more efficient than shown in Figure 7. The number of high-density bodies beyond Neptune may be an indicator of the nature of the largest bodies that once existed – for example, if Earth-mass planets ever roamed there, into which Pluto-mass planets may have collided.

4.2 An Edge Effect

Hit-and-run appears to constitute the majority of collisional outcomes for the large-mass end of randomly excited populations. According to Figure 6, while the largest terrestrial planets eventually did accrete most of the next-largest bodies, they did so on average only after one or more unsuccessful accretion attempts. Dynamically it is true, that planets that collide once, are likely to collide sometime again, but this does not substantially effect the conclusions, since eventually either they accrete and are lost from the population of next-largest bodies, or they don't and survive as hit-and-run remnants. Next-largest bodies that did not grow into or merge into one of the largest bodies suffered events that made them as compositionally exotic as the Moon, which formed in an analogous manner (Figure 5). These are the bodies that are still around.

This is an edge effect, pertaining to the planets that are almost but not quite the largest, by the factor $r/R \approx 1/3$ for which grazing is common in Figure 3. An accreted planet has made it beyond this boundary condition – it has nothing larger to run into. An unaccreted planet finishes its evolution as part of the middle of the pack, but is still located near the upper end of the size distribution (Figure). This means two things:

1. It is among the largest of bodies, and therefore petrologically interesting, potentially thermally active, and (above all) most representative (in terms of mass) of the parent bodies of the final population we see today that are sampled as meteorites.

2. Hit-and-run collisions require impact velocities around the mutual escape velocity.

The second point is perhaps easy to overlook, that SSCs do not occur throughout the size distribution, but primarily between the largest and the next-largest owing to the scaling to v_{eesc}. Figure 6 shows that the hit-and-run line runs through $\xi \approx 0$ for velocities $v_\infty \simeq 0.7$ to 2.5 v_{esc}, which is nominal for a randomly stirred-up population (Agnor *et al.*, 1999). Smaller bodies would also have collisions with bodies of similar size, but at velocities v_∞/v_{esc} far to the right of Figure 6. At these very high normalized velocities hit-and-run survival of major pieces of the impactor does not usually occur. Figure 14 shows results for final impactor mass corresponding to the simulations in Figure 6. Following the trend suggests that for impact velocites faster than about $4-5\,v_{esc}$ very little of the impactor mass survives intact.

4.3 Meteorite origins

The most severe hit-and-run events result in a chain of identifiable planetoids; the largest of them a few times smaller than r. Consider figure 7(d-f), which is not unusually energetic ($v_{imp} = 2\,v_{esc}$), with a 10:1 mass ratio and 30° incidence from normal. The remnants include about a dozen major bodies. Much higher fidelity simulations are required in order to give a far better understanding of their final compositions (iron:rock ratio) and other aspects, but are unlikely to

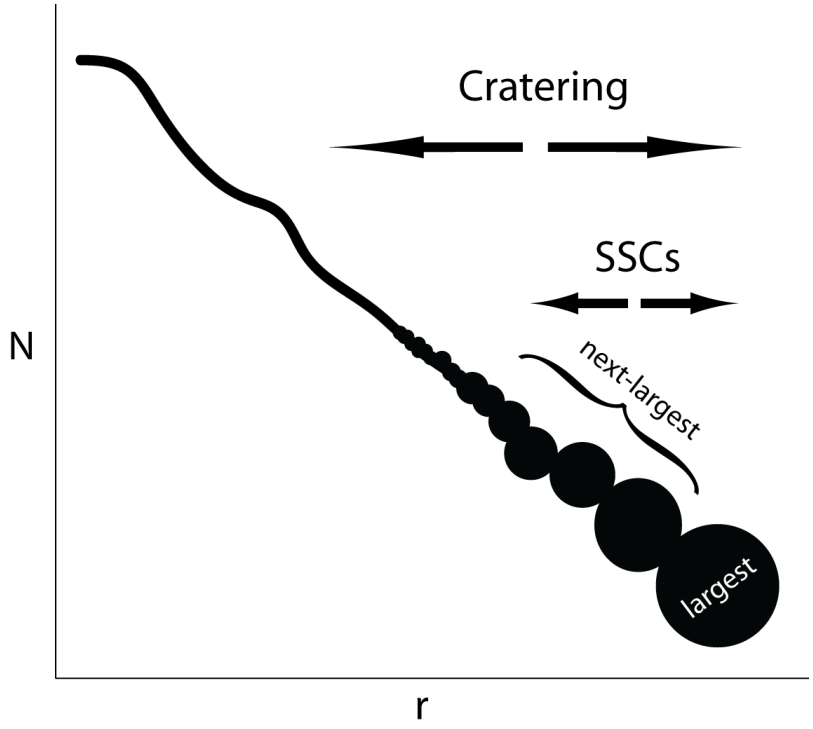

Figure 13: Similar sized collisions occur between the largest and the next-largest bodies in a hierarchically accreting size distribution (see text), shown here schematically as a log-lot plot of cumulative number N versus size r. The next-largest are within a factor of ~ 3 in size of the largest, and their collisions occur at random velocity $v_{esc} \approx v_{\infty}$. For late-stage growth of terrestrial planets, these are called giant impacts, or planet-scale collisions.

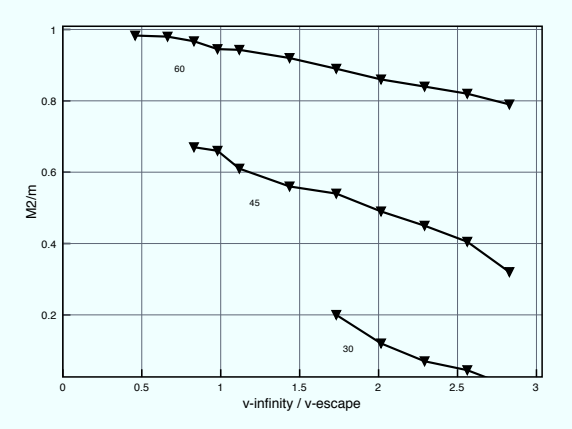

Figure 14: Mass of the largest impactor remnant ($M_2 \leq m$) after a hit-and-run collision, for the 10:1 mass ratio subset of the collisions shown in Figure 6. Calculations by Agnor and Asphaug (2004b). The "missing" points to the left of the graphs for 30° and 45° are events where the impactor and target accrete, so that there is no sizable M_2 (highlighting the abrupt transition from accretion to hit-and-run). To the lower right of the 30° graph there is a gradual transition as $M_2 \rightarrow 0$. Here, although the impactor is unaccreted, any escaping matter is disrupted into small sizes. Inbetween are outcomes, plotted here, that leave behind a substantial portion (or portions) of the impactor mass m. The debris chain that forms in Figure 7(d-f) plots here with a largest fragment mass $M_2 = 0.2\,m$; the outcome is actually several new bodies of about that mass. For the impact angle of 45° the impactor loses between 1/3 and 2/3 its mass in a hit-and-run, as conjectured below for the origin of Mercury.

result in major changes in the number of massive clumps, according to studies of self-gravitational disruptive aftermaths (Asphaug and Benz, 1996) that examined the effect of numerical resolution.

First off, one can make the observation that the surface area of iron to silicate is greatly increased during the event, since the same volume of iron is parceled into many smaller planetoids. Thus, the prevalence of mesosiderites, pallasites, and other iron:silicate mechanical mixtures may be consistent with this type of parent body evolution. When hit-and-run results in the shearing apart of a core body into multiple components, this leads to considerable interplay at the greatly expanded core-mantle interface – where in fact shear localization would be expected to occur, causing detachment and dynamic frictional processes. Second, as mentioned these small bodies are suddenly at much lower lithostatic pressure P_o than they were before, with corresponding potential for degassing, and the fluxing of water or other volatiles, that were originally in pressure equilibrium.

This class of disruptive hit-and-run outcome is perhaps recorded in the IVA iron meteorites and perhaps some other meteorite families. There are dozens of distinct iron meteorite parent bodies, distinguished on the basis of composition (iron and nickel, plus about ten trace metals such as gold). Each iron meteorite reservoir is unique, thus, 14 meteorite groups are widely agreed to represent 14 iron parent bodies. Hundreds of iron meteorites remain unclassified, and by most estimates there are 50 or more iron parent bodies represented by meteorites in our collections. Given the near-impossibility of liberating core iron by a single impact (Figure 1), we consider hit-and-run. According to Ni-Fe metallographic cooling rates Rasmussen *et al.* (1995) the group of IVA irons, one of the major meteorite groups, spans 19–3400 K/Ma, almost 2 orders of magnitude. Yang *et al.* (2007) report revised cooling rates for this group spanning $100 - 6000$ K/Ma, and show a trend for increasing cooling rate with decreasing bulk Ni. In order to satisfy the most rapid cooling rates, and to conform to the Ni data, Yang *et al.* propose a model where the IVA meteorites cooled within a ~ 300 km diameter metallic body that was stripped bare of its mantle, since with an insulating mantle the iron would cool more slowly, and under nearly isothermal conditions.

Stripping a Vesta-sized mantle bare might be possible in a hit-and-run collision, or a succession of hit-and runs as described below. Another way of providing diverse cooling rates to iron meteorites is to rip the core into a new array of planets, each with its own core, its own iron/silicate ratio, its own size, and its own cooling rate. The scenario of Figure 7(d-f) would lead to the formation of a handful of new planets with the same core composition; these would subsequently follow their own evolution as individual minor planets. Meteorites derived from these bodies would come from the same parent body, in terms of core composition and isotopic signatures, but come from different bodies according to cooling and post-formation history.

Without opening up the very broad topic of early solar system origins, it is worth recalling that similar sized collisions are expected to have prevailed since the dawn of asteroid formation, especially if asteroids were born big, but even if they were grown hierarchically. If so, then hot, possibly molten bodies tens to hundreds of km diameter would have undergone collisional evolution

at random speeds comparable to v_{esc}. This SSC scenario would involve "giant impacts" but on a scale that is small compared with Figure 7. These smaller molten asteroids would be pulled apart once or twice for every efficient accretion, as part of the process of growing large bodies from the next-largest. Figure 8 suggests that it might have happened dozens of times to a given parcel of matter. The implications for material processing in the early nebula are significant, and include pressure-unloading and dispersal of materials over $\tau_{grav} \sim$ hours, consistent with the required conditions of chondrule formation. This is the subject of ongoing research into the thermophysical processing of the earliest meteoritic materials from the terrestrial zone.

4.4 Mercury and Mars

Mercury is anomalously iron-rich (about 70% by mass), and Benz *et al.* (1988, 2007) set the removal of Mercury's mantle as an objective for giant impact modeling efforts. They showed that a high energy impact with random velocity $3 - 5 \times v_{esc}$ is capable of shock-accelerating the mantle of Mercury to the extent that $\sim$ 1/2 the mantle escapes the planet. The impactor is The 2007 paper argues that the ejected mantle is fragmented by the impact into sizes small enough to be removed by solar radiation pressure or solar wind effects on short timescale, before it is re-accreted by the planet. Gladman and Coffey (2008) provide dynamical constraints on the latter idea. A compositional critique to the idea is that volatiles in Mercury's crust are abundant enough to drive longstanding episodes of volcanic flows (Denevi *et al.*, 2009); see also (Sprague *et al.*, 1995). It may be difficult to reconcile the presence of crustal magmatic volatiles with the hypothesis that Mercury finished its evolution by being shocked to the extent that half of its mantle was accelerated to $\gtrsim 5$ km/s, dispersed into space, and partially reaccumulated.

Based upon scaling from Figures 6 and 7 a much lower velocity collision would suffice, more comparable to the expected random velocities, if Mercury was the impactor rather than the target. As discussed before, calculations by Wetherill (1992) determined that Mercury could have originated beyond Mars, leading to the possibility of encounters with proto-Earth or proto-Venus. In direct integrations of giant planet migration, and the resulting Saturn-Jupiter commensurability that may be responsible for the late heavy bombardment (the so-called Nice model; Gomes *et al.* 2005), the eccentricity of the smaller planets can grow to become Earth- or Venus-crossing. If Mercury started out Mars-like, it may well have encountered a larger planetary embryo along the way, leading to a planet of roughly Mercury's mass and composition if something like Figure 7(a-c) had occurred. In this simulation the final impator has lost 35% of its original mass ($M_2 = 0.65\, m$), all of it in the form of mantle material, which equals half its mantle. These results for the largest remnant mass are plotted in Figure 14.

It could help to unify our understanding of the dynamics of late stage terrestrial planet formation if Mercury formed in a similar manner to how the Moon formed: a Mars-mass planet striking a

larger planet as in Figure 5, only a little bit faster. The $v_\infty = 0$ impact leaves a protolunar disk and merges the core material (Figure 5); a somewhat faster collision (Figure 7a-c) leaves a planet that has lost half its mantle inventory. This is a topic requiring much further study, since as in the model of Benz *et al.* (2007) the post-impact dynamics and the segregation of ejecta must be considered.

Conclusions

It is taken for granted in most modeling studies of planet formation that colliding planets at random velocities simply merge. This is far from the case, because most of the colliding mass in a hierarchically-accreting planetary system comes in the form of similar sized collisions. SSCs are colliding pairs within a factor of 3 in size that strike at a $v_\infty \approx v_{esc}$, whose geometric sensitivity to incidence angle results in hit-and-run collisions. It is also assumed in models that minor planets can only be disrupted by bodies smaller than themselves. This is also not the case: the next-largest planets (those a factor of ~ 3 smaller than the largest, for instance the fossil Main Belt when it contained Moon-sized bodies) are disrupted by the largest planets as frequently as they are accreted by them. This leaves behind a large population of hit-and-run disrupted planetoids.

There is great diversity among terrestrial planets that are a few times smaller than the largest (Mars, Mercury and smaller). This can be understood as an edge effect in the size distribution: if a planet becomes one of the largest bodies then it has nothing larger to collide *into*. "Accreted" planets become amalgams of their feeding zones (e.g. Chambers and Wetherill, 1998), and although impacts by smaller bodies batter their outer layers, removing atmophiles and in some cases removing much of their crust (Figure 1 (see also Nimmo *et al.*, 2008; Marinova *et al.*, 2008). Removal of their outer mantles requires impacts with energy well to the right of what is plotted in Figure 6 (for example, $v_\infty \approx 8\, v_{esc}$ and $r \approx R/2$ in the Mercury-stripping simulations of Benz *et al.* (2007). The cores and deep mantles of accreted planets are undisruptable.

Unaccreted planets are quite different. They evolve to their finished size within a population that includes bodies that are a few times larger than themselves. They are lucky survivors: for every one of the next-largest bodies that survives the tumultuous first ∼billion years, there are $\sim 10 - 100$ others that have become integrated with the larger bodies (for a $\beta \approx 2$ distribution). In terms of Figure 6 the picture is not quite hit-or-miss; there is a tremendous sensitivity to impact parameter that leads to a lot of shredded planets – big ones – before there will be a lot of accretion.

Hit-and-run collisions can strip off outer layers and crusts without even impacting ($\theta = 90°$). With a moderately deep but glancing blow, a Moon-mass planet can be torn by a Mars-mass planet (Figure 7d-f) into a chain of kindred bodies, each a few times the mass of Vesta, and of highly diverse composition. The bulk density of surviving (unaccreted) "next-largest" bodies increases significantly during this epoch, as the atmospheres, crusts and mantles are stripped away. They

also are processed globally during episodes of planet-scale pressure unloading, something that is a major feature of grazing collisions (Figure 11). During the event that scattered large differentiated ice-rock dwarf planets beyond Neptune, hit-and-run collisions are also likely to have occurred, depending on the preponderance of any larger bodies that may have once existed.

The hypothesis is an extension of models for the Moon's formation, which appears almost to have been a hit-and-run collision, according to models. It applies to Mercury, which seems perhaps more likely to have shed its mantle in a low-v_∞ glancing blow with proto-Earth or proto-Venus during an early stage or later chaos – an event closely akin to the Moon's formation – than to have had it blasted off by an unusually high velocity impact. In our solar system, the Main Belt asteroids would consist largely of the relics from such a process, if planet-sized parent bodies once were part of the collisional population between Mars and Jupiter. There is direct evidence for this process in the diverse cooling rates of iron meteorites (Yang *et al.*, 2007), and indirect evidence in the wide diversity of meteorite parent bodies, including hydrothermally altered and metamorphosed systems (Keil, 2000) and the preponderance of iron and iron-silicate varieties. The hypothesis predicts a heterogeneous and complex record, because the largest scale collisions are the most stochastic. Some unaccreted bodies (Vesta) may have avoided hit-and-run collisions entirely, while others (bare metallic remnants like Kleopatra) could have experienced several.

One of the more important corollaries of this hypothesis pertains to extasolar planetary systems with super-Earths (see e.g. Ribas *et al.*, 2008). In these systems, it is the Earth-mass planets, an order of magnitude less massive than the super-Earths, that have survived unaccreted. In these solar systems the "Earths" are expected to exhibit as wide of a range of compositional diversity, as the smaller terrestrial planets do in our own solary system. This hypothesis predicts Earth-mass planets devoid of crusts and atmospheres, and varying by half or more in bulk density, based on simple analogy with our own planetary system which shows tremendous diversity in its next-largest planets, which are the sources of most meteorites.

Acknowledgements

This research was sponsored in equal part by NASA's Planetary Geology & Geophysics Program ("Small Bodies and Planetary Collisions") and Origins of Solar Systems Program ("Meteorite and Dynamical Constraints on Planetary Accretion") under Research Opportunities in Space and Earth Sciences. This work has emerged from collaborations spanning 15 years with Willy Benz, Robin Canup and others, especially three years working with Craig Agnor, with whom most of the featured calculations were performed. I am grateful to Ed Scott, Quentin Williams, Jeff Cuzzi and Naor Movshovitz for insightful ideas and ongoing critical discussions, and to Klaus Keil for his original thinking on igneous and evolved asteroids and for inviting me to write this review. But I am solely responsible for any errors or omissions or outlandish claims.

References

Agnor, C., and E. Asphaug, 2004a, The Astrophysical Journal **613**, L157.

Agnor, C., and E. Asphaug, 2004b, AGU Fall Meeting Abstracts , A2+.

Agnor, C. B., R. M. Canup, and H. F. Levison, 1999, Icarus **142**, 219.

Alidibirov, M., and D. B. Dingwell, 1996, Nature **380**, 146.

Asphaug, E., 1997, Meteoritics and Planetary Science **32**, 965.

Asphaug, E., and C. Agnor, 2005, in *Bulletin of the American Astronomical Society*, volume 37 of *Bulletin of the American Astronomical Society*, pp. 623–+.

Asphaug, E., C. B. Agnor, and Q. Williams, 2006, Nature **439**, 155.

Asphaug, E., and W. Benz, 1994, Nature **370**, 120.

Asphaug, E., and W. Benz, 1996, Icarus **121**, 225.

Asphaug, E., and H. J. Melosh, 1993, Icarus **101**, 144.

Benz, W., 2000, Space Science Reviews **92**, 279.

Benz, W., A. Anic, J. Horner, and J. A. Whitby, 2007, Space Science Reviews **132**, 189.

Benz, W., and E. Asphaug, 1999, Icarus **142**, 5.

Benz, W., A. G. W. Cameron, and H. J. Melosh, 1989, Icarus **81**, 113.

Benz, W., W. L. Slattery, and A. G. W. Cameron, 1988, Icarus **74**, 516.

Bizzarro, M., J. A. Baker, H. Haack, and K. L. Lundgaard, 2005, The Astrophysical Journal **632**, L41.

Bottke, W. F., D. D. Durda, D. Nesvorný, R. Jedicke, A. Morbidelli, D. Vokrouhlický, and H. Levison, 2005, Icarus **175**, 111.

Burton, M. R., T. Caltabiano, F. Murè, G. Salerno, and D. Randazzo, 2009, Journal of Volcanology and Geothermal Research **182**, 214.

Cameron, A. G. W., and W. Benz, 1991, Icarus **92**, 204.

Canup, R. M., 2004, Annual Review of Astronomy and Astrophysics **42**, 441.

Canup, R. M., and E. Asphaug, 2001, Nature **412**, 708.

Chambers, J. E., 2007, Icarus **189**, 386.

Chambers, J. E., and G. W. Wetherill, 1998, Icarus **136**, 304.

Chambers, J. E., and G. W. Wetherill, 2001, Meteoritics and Planetary Science **36**, 381.

Chandrasekhar, S., 1969, *Ellipsoidal figures of equilibrium* (The Silliman Foundation Lectures, New Haven: Yale University Press, 1969).

Cuzzi, J. N., R. C. Hogan, and K. Shariff, 2008, Astrophysical Journal **687**, 1432.

Denevi, B. W., M. S. Robinson, S. C. Solomon, S. L. Murchie, D. T. Blewett, D. L. Domingue, T. J. McCoy, C. M. Ernst, J. W. Head, T. R. Watters, and N. L. Chabot, 2009, Science **324**, 613.

Desch, S. J., and H. C. Connolly, Jr., 2002, Meteoritics and Planetary Science **37**, 183.

Dixon, J. E., E. Stolper, and J. R. Delaney, 1988, Earth and Planetary Science Letters **90**, 87.

Dohnanyi, J. W., 1969, Journal of Geophysical Research **74**, 2531.

Dominik, C., J. Blum, J. N. Cuzzi, and G. Wurm, 2007, in *Protostars and Planets V*, edited by B. Reipurth, D. Jewitt, and K. Keil, pp. 783–800.

Gardner, J. E., M. Hilton, and M. R. Carroll, 1999, Earth and Planetary Science Letters **168**, 201.

Ghosh, A., S. J. Weidenschilling, H. Y. McSween, Jr., and A. Rubin, 2006, *Asteroidal Heating and Thermal Stratification of the Asteroidal Belt* (Meteorites and the Early Solar System II), pp. 555–566.

Gladman, B. J., and J. Coffey, 2008, LPI Contributions **1405**, 8289.

Gomes, R., H. F. Levison, K. Tsiganis, and A. Morbidelli, 2005, Nature **435**, 466.

Grady, D. E., and M. E. Kipp, 1985, Journal of Applied Physics **58**, 1210.

Hahn, J. M., and T. W. Rettig, 2000, Icarus **146**, 501.

Head, J. N., H. J. Melosh, and B. A. Ivanov, 2002, Science **298**, 1752.

Jeffreys, H., 1947, Monthly Notices of the Royal Astronomical Society **107**, 260.

Johansen, A., J. S. Oishi, M.-M. M. Low, H. Klahr, T. Henning, and A. Youdin, 2007, Nature **448**, 1022.

Kamenetsky, V. S., M. B. Kamenetsky, V. V. Sharygin, and A. V. Golovin, 2007, Geophysical Research Letters **34**, 9316.

Keil, K., 2000, Planetary and Space Science **48**, 887.

Kelley, S. P., and J.-A. Wartho, 2000, Science **289**, 609.

Kokubo, E., and S. Ida, 1998, Icarus **131**, 171.

Leinhardt, Z. M., D. C. Richardson, and T. Quinn, 2000, Icarus **146**, 133.

Levison, H. F., and A. Morbidelli, 2003, Nature **426**, 419.

Marcus, R. A., S. T. Stewart, D. Sasselov, and L. Hernquist, 2009, Astrophysical Journal Letters **700**, L118.

Marinova, M. M., O. Aharonson, and E. Asphaug, 2008, Nature **453**, 1216.

Melosh, H. J., 1989, *Impact cratering: A geologic process* (Research supported by NASA. New York, Oxford University Press (Oxford Monographs on Geology and Geophysics, No. 11), 1989, 253 p.).

Melosh, H. J., E. V. Ryan, and E. Asphaug, 1992, Journal of Geophysical Research **97**, 14735.

Merk, R., D. Breuer, and T. Spohn, 2002, Icarus **159**, 183.

Morbidelli, A., W. Bottke, D. Nesvorny, and H. F. Levison, 2009, ArXiv e-prints `0907.2512`.

Nimmo, F., S. D. Hart, D. G. Korycansky, and C. B. Agnor, 2008, Nature **453**, 1220.

Petit, J.-M., A. Morbidelli, and J. Chambers, 2001, Icarus **153**, 338.

Pierazzo, E., and H. J. Melosh, 1999, in *Lunar and Planetary Institute Conference Abstracts*, volume 30 of *Lunar and Planetary Institute Conference Abstracts*, pp. 1223–+.

Porritt, L. A., and R. A. F. Cas, 2009, Journal of Volcanology and Geothermal Research **179**, 241.

Rasmussen, K. L., F. Ulff-Møller, and H. Haack, 1995, Geochimica et Cosmochimica Acta **59**, 3049.

Ribas, I., A. Font-Ribera, and J.-P. Beaulieu, 2008, Astrophysical Joural Letters **677**, L59.

Roche, E., 1850, La figure d'une masse fluide soumise a l'attraction d'un point éloginé.

Safronov, V. S., and E. V. Zvjagina, 1969, Icarus **10**, 109.

Schäfer, C., R. Speith, and W. Kley, 2007, Astronomy and Astrophysics **470**, 733.

Schenk, P. M., E. Asphaug, W. B. McKinnon, H. J. Melosh, and P. R. Weissman, 1996, Icarus **121**, 249.

Scott, E. R. D., H. Haack, and S. G. Love, 2001, Meteoritics and Planetary Science **36**, 869.

Shoemaker, E. M., 1962, *Physics and Astronomy of the Moon* (Academic Press), chapter Interpretation of Lunar Craters, pp. 283–351.

Sprague, A. L., D. M. Hunten, and K. Lodders, 1995, Icarus **118**, 211.

Sridhar, S., and S. Tremaine, 1992, Icarus **95**, 86.

Stevenson, D. J., 1987, Annual Review of Earth and Planetary Sciences **15**, 271.

Tackley, P. J., 2001, Journal of Geophysical Research **106**, 32971.

Walzer, U., R. Hendel, and J. Baumgardner, 2004, Tectonophysics **384**, 55.

Warren, P. H., 1994, Icarus **111**, 338.

Wasserburg, G. J., and D. A. Papanastassiou, 1982, in *Essays in Nuclear Astrophysics*, pp. 77–+.

Weibull, W., 1939, **151-3**, 45.

Weissman, P. R., E. Asphaug, and S. C. Lowry, 2004, Comets II , 337.

Wetherill, G. W., 1980, Annual Review of Astronomy and Astrophysics **18**, 77.

Wetherill, G. W., 1985, Science **228**, 877.

Wetherill, G. W., 1992, Icarus **100**, 307.

Wilson, L., and K. Keil, 1991, Earth and Planetary Science Letters **104**, 505.

Wurm, G., and J. Blum, 2006, *Experiments on planetesimal formation* (Planet Formation), pp. 90–+.

Yang, J., J. I. Goldstein, and E. R. D. Scott, 2007, Nature **446**, 888.

Yin, Q., S. B. Jacobsen, K. Yamashita, J. Blichert-Toft, P. Télouk, and F. Albarède, 2002, Nature **418**, 949.